ISSN: online 2709-2666
print 2663-7006

AZERBAIJAN JOURNAL OF CHEMICAL NEWS

Vol. 6, No.1, 2024

Abstracting and indexing

Journal is indexed in Crossref, İndex Copernicus, Scilit and E-library

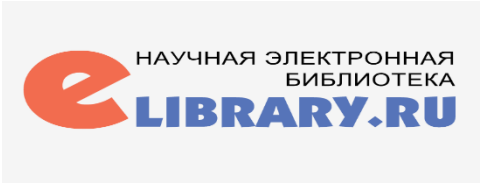

Azerbaijan Journal of Chemical News

ISNN: print 2663-7006; online 2709-2666

Azerbaijan Journal of Chemical News

CONTENT

ISNN: print 2663-7006; online 2709-2666

AJCN, Vol. 6, No. 1, 2024, pp.4-10
https://doi.org/10.32010/AJCN04022024-4

UDC 622:504.5

STUDY OF ECOTOXICANTS IN THE DISCHARGE OF MINING WASTEWATER IN OKCHUCHAY

[1]*S.R.Hajiyeva*[0009-0005-3444-9038], [2]*İ.İ.Mustafayev*[0009-0004-0570-5517],
[1]*A.A.Samadova*[0009-0008-2758-820X], [3]*R.Abdullayeva*[0009-0009-2977-2200]
[1]*Baku State University,* [2] *Institute of Radiation Problems*
[3]*The Ministry of Ecology and Natural Resources*
aytensamadova@bsu.edu.az

If we do not take environmental norms and standards into account, it can cause serious damage to the environment and can have negative consequences because of the mining industry. As a result of the usage of the Akarek copper-molybdenum resources, the solid and liquid forms of wastes are a threat to the ecology. Armenia's mining industry has caused ecological imbalance in the region. The waste of the copper-molybdenum deposit in the city of Gajaran continues to pollute Okchuchay. As a result of the fact that the river is a tributary of the Araz River, it has polluted the land and water resources in the region to a dangerous level. An environmental assessment of Okchuchay, which was polluted by the waste water of the mining industry, was carried out. The distribution dynamics of heavy metals were investigated. Conducting ecological monitoring on the water course, the influence of environmental factors on this spread has been studied. In particular, the effect of physical environmental factors on the speed of this pollution has been clarified. The conducted research clearly shows that the quality of water in the river systems that pass through the mining industry regions of Armenia does not follow international standards for domestic use and irrigation. Direct or indirect pollution of border rivers such as the Kura and Araz rivers can be also considered as a serious threat to the ecology of the entire Caspian basin. This shows that the problem has already become global. Establishing a scientific basis for mining and environmental monitoring, the acceptable level of impact for the elements of the biosphere and ecological systems which are capable of self-cleaning, self-recovery and development, establishment of a network of stations in order to gain information on the natural resources of these systems have a huge importance. For elements of the biosphere and ecological systems that are not capable of self-cleaning and self-repair, their protection also has a particular significance. The study on the environmental conditions in terms of its influence on human health should be enormously vital.
Keywords: *ecotoxicant, ecology, mining industry, Okchuchay, heavy metals, environmental monitoring, anion, cations, natural and drinking water.*

INTRODUCTION

The Karabakh territory, which has undergone ecological changes, is already showing its consequences. Due to the environmental terrorism and environmental vandalism of Armenians, Okchuchay is now seriously polluted with organic and inorganic substances. They are 1989 - Basel Convention (Control of Transboundary Movement and Disposal of Hazardous Waste), 1999 - Basel Convention (Control of Transboundary Movement and Disposal of Hazardous Waste), 1991 - Expo Convention, Finland (Convention on Environmental Impact Assessment in a Transboundary Context), 1992 Helsinki Convention (Protection and Use of Transboundary Watercourses and International Lakes) do not comply with internationally signed documents. The state of Armenia has caused problems in the International

environmental policy on fulfilling the requirements of the Environmental Impact Assessment Conventions in the international Transboundary context [1].

It should be noted that one of the most polluting rivers of Araz is Okchuchay. Hundreds of thousands of tons of solid sour waters, heavy metal salts and other wastes from Megri, Gajaran, Gafan and Dastekert mining (metallurgical) combines have excessively polluted Okchuchay. At different times, the amount of copper in the water was 25-50 times the permissible concentration limit, and the amount of phenyls regularly exceeded the norm by 6-15 times. Aluminum, zinc, manganese, titanium and bismuth polluting elements are constantly found in Okchuchay. It is known that heavy metals have cumulative and toxic properties [2-6]. New scientifically based methods for cleaning pollutants should be proposed. The use of sorbents has a definitely great importance for cleaning natural water sources contaminated with heavy metals (especially cobalt, lead, chromium, copper, etc.). Thus, they have natural alternatives in nature - sorbents, which can be chosen based on the principle of convenience. These processes might create an opportunity for both the health of the sututars and the ecological assessment of the environment. At the same time, it is economically viable. As a consequence of it, the development of these new methods can be considered both ecologically and economically relevant.

EXPERIMENTAL PART

The composition and structure of water samples taken from the Okchuchay River located in the Karabakh region were studied in detail by IR-spectroscopy, chromatography, mass spectrometry and AAS methods. The composition of water samples was made by comparative analysis. The dynamics of changes in properties with an interval of up to 3 months were observed by physico-chemical methods. The laws of transformation of existing heavy metals have been studied. The dynamics of change as a result of the influence of environmental factors were investigated. Comparative analyzes of natural sorbents were carried out for the elimination of water pollution. In water samples for comparative analysis, anions (nitrate ion NO_3-, nitrite ion NO_2-, carbonate ions, chlorides, sulfates, etc.), cations (especially chromium-Cr, manganese-Mn, iron-Fe, copper-Cu, nickel -Ni, cadmium-Cd, lead-Pb, zinc-Zn, molybdenum-Mo, cobalt-Co, aluminum-Al, arsenic-As, selenium-Se, tin-Sn, etc.) were studied [7-10]. For comparison, analyzes were conducted with an interval of one, two, three months. At the same time, the time-dependent change of these cations and anions in water was studied. The effect of environmental factors on them was investigated. Research of new methods will be conducted to eliminate those compounds. For this reason, natural sorbents were used first. In this way, the most ecologically and economically optimal way of reducing the pollutants of the water environment will be selected.

RESULTS AND DISCUSSION

As we noted, on 12.06.2023, ecological monitoring of the upper, medium, and lower streams was conducted to evaluate the environmental impact of Okchuchay from rivers contaminated with waste water. For this reason, we collected water samples from the region of Okchuchay, in the upper part of the country the Upper Stream, the Middle Stream, the Shayifli, and the lower stream [11, 12]. The GPS coordinates of the areas where we took the samples are given in table1.

ISNN: print 2663-7006; online 2709-2666

Table 1

Coordinates where the samples were taken

№	Territories	Coordinates	
1	Burunlu	$39^0 02' 43.1''$	$46^0 44' 09.0''$
2	Shayifli	$39^0 07' 19.1''$	$46^0 34' 19.7''$
3	Jahangirbeyli	$39^0 10' 23.5''$	$46^0 30' 39.8''$

In the water samples taken from the upper, middle and lower streams of Okchuchay, respectively, a pH-meter for pH-hydrogen indicator, an oximeter for dissolved oxygen, a conductometer for electrical conductivity, an autotitrator for sodium and chloride ions, a spectrometer (Specord 205, Hitachi UH 5300) for sulfate, ammonium, nitrite, nitrate ions, and metals were determined in the optical emission and atomic absorption spectrometer (İCP OES-GBC Quantima, AAS-700 Shimadzu)
The results of physical parameters are showed in table 2.

Table 2

Results of the physical parameters of water samples taken from the Okchuchay region on 12-14.06.2023

	Name of components	Unit of measure-ment	Amount of components			Permissible viscosity limits
			Okchuchay-Zengilan village			
			Jahangir beyli village	Shayifli village	Burunlu village	
1	Hydrogen indicator, pH	–	7.2	7.3	7.3	6.5-8.5
2	Dissolved oxygen	mqO_2/l %	7.3 75.0	7.2 76.0	6.1 64.0	≥4.0
3	Electrical conductivity	µSm/sm	496	456	470	–
4	Codiness	mq-ekv/l	4.47	3.89	4.25	7.0

After the physical parameters were assigned to the aforementioned devices, we assigned the anion and cations contained in it with ICP OES-GBC Quantima, AAS-700 Shimadzu, Specord 205 branded spectrometer, and Hitachi UH 5300. The results of the assignment are listed in table 3.

Table 3

Analysis results of water samples taken from the territory of Eastern Zangezur and Karabakh economic region on 12-14.06.2023

№	Name of components	Unit of measure-ment	Amount of components			Permissible viscosity limits
			Okchuchay-Zengilan village			
			Jahangir beyli village	Shayifli village	Burunlu village	
1	2	3	4	5	6	7
1	Chloride ion , Cl^-	mq/l	15.1	11.9	12.0	350
2	Sulfate ion, SO_4^{2-}	mq/l	147.2	133.0	136.0	500
3	Ammonium ion, NH_4^+	mq/l	0	0	0	0.5

Cont. of table 3

4	Nitrite ion, NO_2^-	mq/l	0.01	0.27	0.36	3.3
5	Nitrate ion, NO_3^-	mq/l	6.4	6.0	5.7	45.0
6	Cyanides	mq/l	0	0	0	0.1
7	Copper , Cu	mkq/l	73.1	81.7	94.1	1000
8	Iron, Fe	mkq/l	515.0	705.0	735.0	300
9	Manganese , Mn	mkq/l	138.0	170.0	174.0	100
10	Lead, Pb	mkq/l	8.70	9.75	15.2	30
11	Zink, Zn	mkq/l	54.9	65.5	71.5	1000
12	Nickel, Ni	mkq/l	0.739	1.39	1.43	100
13	Molybdenum , Mo	mkg/l	33.7	44.4	46.7	250

The Permissible Hardness Limits (PRLs) for surface water are taken from the document "Rules for the protection of surface water from pollution by waste water" approved by the State Ecology and Nature Use Control Committee of the Republic of Azerbaijan by order No. 01 of January 4, 1994.

As it is shown in the table, according to the analyzes conducted on water samples, iron (Fe) - 1.7 times in the village of Jahangirbeyli in Okchuchay, 2.4 times in the village of Shayifli, 2.5 times higher in the village of Burunlu, apart from that, manganese (Mn) - 1.4 times higher in the village of Jahangirbeyli in Okchuchay and 1.7 times higher in the villages of Shayifli and Burunlu.

CONCLUSION

It is well known that too much iron entering the body through water causes a general toxic effect that lowers the gastrointestinal sequence and impairs liver function. Additionally, oxygen, which is solved in two-dimensional iron water, is easily oxidized and becomes three-dimensional. Therefore, oxygen starvation causes mass destruction of fish and other hydrobiants. At the same time, Mo accelerates oxidation and nitrogen exchange, including vital ultramicroelement, a number of enzymes. The excess amount of molybdenum in the organism has an undeniably negative effect on the metabolism of calcium and phosphates. At the same time, molybdenum accelerates the synthesis of carbohydrates (2,6.8-trioxipurin), which might cause stones in the kidneys. Too much presence of manganese, on the other hand, accumulates in bones and muscles and lead them to gradual destruction [13-17].

Based on the information provided, it can be said that parameters that are higher than the allowable concentration limit seriously harm living organisms. It should be taken into account that the processes and events that occur in the environment during the usage of mineral deposits are quite diverse. The speed of these processes and events can be catastrophically high from zero in their extreme values, . Accordingly, there may be dramatic changes in a person's health or in other cases less noticeable changes, but this can lead to chronic diseases as well.

REFERENCES

1. Hajiyeva S.R., Aliyeva F.S.The true face of aggression: Through injustige and blooshed- Ecological terror in Nagorno-Karabakh. 2021, pp.99-111
2. Filov V.A. Chemical pollutants of the environmental, toxicology and information

ISNN: print 2663-7006; online 2709-2666

issues. Ros.chem. journal. 2004, T.48, № 2, pp. 4-8
3. Medvedev I.F., Derevyagin S.S. Heavy metals in ecosystem, Saratov.: «Rakursc». 2017. pp.178
4. Davidova S.L. About the toxicity of metal ions, Series "Chemistry"№3, 1991, pp. 243
5. Mur J. V., Ramamurti S. Heavy metals in natural waters. M.: Mir, 1987. pp. 297.
6. Mudriy I.V. Heavy metals in the soil plant human system. Hygiene and sanitation–Moscow. 1997, № 1. pp.14-16
7. Hajiyeva S.R.,Valiyeva Z.T., Aliyeva T.İ., Jafarova N.M. Chemical ecotoxicology 2021,pp. 73-95
8. Drinking water. Methods of determining content Pb, Zn, Ag: GOST 18293-72. - M.: State Committee of the USSR on standards. 1980, pp. 19
9. Lurye U.U. Handbook of analytical chemistry. M.: Chemistry. 1979.pp.480.
10. Korostilev P.P. Preparation of solutions for chemical and analytical works.M.: Nauka.1981, pp. 202
11. Hajiyeva S.R., Shamilov N.T., Aliyeva T.İ., Samadov J.Z., Samadova A.A. Practical works of ecological monitoring. 2019, pp. 113-117
12. https://azertag.az/xeber/Oxchuchayin_chirklenme_gostericileri_arasdirilib-2412557
13. Shachneva E.U. Impact of heavy toxic metals on the environment .Scientific potential of regions for the service of modernization. 2012, № 2 (3), pp. 127-134
14. Drinking water. Taken of sample: GOST 24481-80. M.: State Committee of the USSR on standards, 1986. pp.4
15. Hajiyeva S.R., Huseynov F.E., Veliyeva Z.T. Ecological chemistry. 2018, pp.43-48
16. Charikov A.K. Mathematical processing of results of chemical analysis L.: Chemistry 1984, pp. 168
17. Hajiyeva S.R., Aliyeva F.S., Mardanova V.İ., Valiyeva Z.T. Fundamentals of ecotoxicology. 2019, pp.123-136

This work was carried out with the financial support of the Azerbaijan Science Foundation- **Grant №AEF-MQM-QA-1-2021-4(41)-8/07/4-M-07**

ИЗУЧЕНИЕ ЭКОТОКСИКАНТОВ В СБРОСЕ СТОЧНЫХ ВОД ГОРНОДОБЫВАЮЩЕЙ ПРОМЫШЛЕННОСТИ НА ОКЧУЧУ

[1]С.Р.Гаджиева[0009-0005-3444-9038], [2]И.И.Мустафаев[0009-0004-0570-5517],
[1]А.А.Самедова[0009-0008-2758-820X], [3]Р.З.Абдуллаева[0009-0009-2977-2200]
[1] Бакинский Государственный Университет
[2] Институт Радиационных Проблем
[3]Министерство Экологии и Природных Ресурсов
aytensamadova@bsu.edu.az

Горнодобывающая промышленность, которая осуществляется без соблюдения каких-либо экологических норм и стандартов, наносит серьезный ущерб окружающей среде и создает экологические последствия. Твердые и жидкие отходы, сбрасываемые в реки, в результате эксплуатации Акарекского медно-молибденового месторождения, представляют угрозу для экологии. Горнодобывающая промышленность Армении разрушает экологический баланс в регионе. Окчучай продолжают загрязнять отходы

медно-молибденового месторождения, эксплуатируемого в городе Гаджаран. В результате река, являясь притоком реки Араз, до опасного уровня загрязнила земельные и водные ресурсы региона. Проведена экологическая оценка Окчучая, загрязненного сточными водами горнодобывающей промышленности. Исследована динамика распределения тяжелых металлов. Проводя экологический мониторинг на водотоке, изучено влияние факторов окружающей среды на это распространение. В частности, выяснено влияние физических факторов окружающей среды на скорость этого загрязнения. Проведенные исследования позволяют сказать, что качество воды в речных системах нашей страны, проходящих через горнодобывающие районы Армении, не соответствует международным стандартам для бытового использования и применения в ирригации. Прямое или косвенное загрязнение приграничных рек, таких как Кура и Араз, также представляет серьезную угрозу экологии всего Каспийского бассейна. Это показывает, что проблема уже приобрела глобальный масштаб. Имеет большое значение создание научной основы горно-экологического мониторинга участка биосферы, затронутого добычей полезных ископаемых, а также создание сети контрольных пунктов для получения информации для изучения допустимого уровня воздействия на элементы биосферы и экологические системы, способные к самоочищению, самовосстановлению и развитию, о природных ресурсах этих систем и уровне их эффективного использования. Для элементов биосферы и экологических систем, не способных к самоочищению и самовосстановлению, особое значение имеет их охрана и рациональное использование. Важное место должно занять изучение состояния окружающей среды с точки зрения ее влияния на здоровье человека.
Ключевые слова: *экотоксикант, экология, горнодобывающая промышленность, Окчучай, тяжелые металлы, экологический мониторинг, анионы, катионы, природная и питьевая вода.*

OXÇUÇAYA AXIDILAN DAĞ-MƏDƏN SƏNAYESİNİN TULLANTI SULARINDA EKOTOKSİKANTLARIN TƏDQİQİ

[1]S.R.Hacıyeva[0009-0005-3444-9038], [2]İ.İ.Mustafayev[0009-0004-0570-5517],
[1]A.A.Səmədova[0009-0008-2758-820X], [3]R.Z.Abdullayeva[0009-0009-2977-2200]
[1] Bakı Dövlət Universiteti, [2] Radiasiya Problemləri İnstitutu
[3] Ekologiya və Təbii Sərvətlər Nazirliyi
aytensamadova@bsu.edu.az

Heç bir ekoloji norma və standartlar gözlənilmədən aparılan dağ-mədən sənayesi işlərində ətraf mühitə ciddi zərər vurur, ekoloji fəsadlar yaranır. Əkərək mis-molibden yatağının istismarı nəticəsində də çaylara axıdılan bərk və maye tullantılar ekologiyaya təhlükə yaratmaqdadır. Ermənistanın dağ-mədən sənayesi regionda ekoloji balansın pozulmasına səbəb olub. Qacaran şəhərində istismar edilən mis-molibden yatağının tullantıları Oxçuçayı çirkləndirməyə davam edir. Nəticədə çay Araz çayının qolu olması, regiondakı torpaq sahələrinin və su resurslarının təhlükəli həddə çatacaq qədər çirkləndirib. Dağ-mədən sənayesinin tullantı suları ilə çirklənməyə məruz qalmış Oxçuçayın ekoloji qiymətləndirilməsinin aparılması bu baxımdan önəmlidir. Ağır metalların yayılma dinamikası araşdırılması, ekoloji monitorinqlərin su axını üzrə aparılması, ətraf mühit faktorlarının bu yayılmaya təsirinin tədqiq edilməsi mühüm olmuşdur. Xüsusilə fiziki ekoloji faktorların bu çirklənmənin sürətinə təsiri aydınlaşdırılmalı idi. Aparılan tədqiqatlar onu deməyə əsas verir ki, Ermənistanın mədən sənayesi bölgələrindən keçərək ölkəmizə daxili olan çay sistemlərində suyun keyfiyyəti, məişətdə istifadəsi və irriqasiyada tətbiqi üçün beynəlxalq standartlara uyğun deyil. Kür və Araz çayı kimi sərhədyanı çayların birbaşa və ya dolayı yolla çirkləndirilməsi həm də bütün Xəzər hövzəsinin ekologiyasına ciddi təhdid yaradır. Bu isə, problemin artıq qlobal miqyasa keçdiyini göstərir. Biosferin mədənçıxarmanın təsirinə məruz qalan hissəsinin mədən

ISNN: print 2663-7006; online 2709-2666

və ətraf mühitin monitorinqi üçün elmi əsasların yaradılması, biosferin elementləri və özünütəmizləmə, özünü bərpa və inkişaf etdirməyə qadir olan ekoloji sistemlər üçün təsirin məqbul səviyyəsi, bu sistemlərin təbii ehtiyatlarına və onlardan səmərəli istifadə səviyyəsinə dair məlumat əldə etmək üçün idarəetmə məntəqələri şəbəkəsinin yaradılması böyük əhəmiyyət kəsb edir. Biosferin və ekoloji sistemlərin özünütəmizləmək və özünütəmir etmək qabiliyyəti olmayan elementləri üçün onların mühafizəsi və rasional istifadəsi xüsusi əhəmiyyət kəsb edir. Ətraf mühitin vəziyyətinin insan sağlamlığına təsiri baxımından öyrənilməsi mühüm yer tutmalıdır.
Açar sözlər: *ekotoksikant, ekologiya, dağ-mədən sənayesi, Oxçuçay, ağır metallar, ekoloji monitorinq, anion, kationlar, təbii və içməli su.*

AJCN, Vol. 6, No. 1., 2024, pp.11-20
https://doi.org/10.32010/AJCN04022024-11

UDC: 543.8

SYNTHESIS AND STRUCTURE OF NEW COMPLEXES BASED ON SILVER NANOPARTICLES, BISACETYLACETONETHYLENEDIIMINE REAGENT AND CETYLTRIMETHYLAMMONIUM BROMIDE

A.A.İmamaliyeva [0009-0005-5942-2608], *F.V.Hajiyeva* [0000-0003-1686-3401], *F.M.Ciraqov* [0000-0002-2677-9046]
Baku State University
aytenimamaliyeva@hotmail.com

This article provides a comprehensive review of the relationship between azo reagents and silver nanoparticles (AgNP), highlighting significant advances in analytical chemistry and materials science. The integration of silver nanoparticles with azo compounds has shown remarkable improvements in sensitivity, selectivity, and catalytic activity, leading to new applications in various fields. The article highlights the principles of ultraviolet spectroscopy (UV), discusses experimental methodologies, and elucidates the insights gained into the nature of the complexes formed between silver nanoparticles and azo compounds. Today, the synthesis of silver nanoparticles is widespread due to their many applications in various fields. In the presented article, silver nanoparticles were obtained by the green synthesis method. At the same time, the bisacetylacetonethylenediimine (R) reagent was synthesized and new complexes of nanoparticles were synthesized based on the cetylacetonethylenediimine (CTAB) reagent and acetyl trimethylammonium bromide. The complexes were investigated by UV spectroscopy and the optimal formation conditions were determined. It was determined that the optimal formation of the complex is observed at concentrations of 0.01 M of silver nanoparticles, 10^{-3} M of the reactant, and 0.5% of the surfactant. UV analysis of the synthesized complexes was conducted, and it was determined that the R reagent gives a maximum peak at the wavelength of 223 nm, 270 nm, 299 nm. During the UV study of the synthesized complexes, it was determined that the binary complex is 227 nm, 272 nm, 308 nm, and the maximum wavelength of the peaks of the ternary complex formed by adding CTAB as a stabilizer is 214 nm, 243 nm, 285 nm.
Keywords: *silver, nanoparticle, CTAB, complex, reagent.*

INTRODUCTION

Silver (Ag) nanoparticles have been intensively studied in recent years due to their potential application in bio diagnostics, visualization, biological marking, sensing, analytical determination, and other fields. Nanoparticles have been the center of intensive research not only because of their new properties, which are very different from other substances, but also because of their wide application in the modern world [1,2]. Nanoparticles are incorporated into coatings that absorb solar energy and they are used as catalysts for chemical reactions, in the production of highly effective substrates, and as antimicrobial agents and disinfectants. Ag nanoparticles have unusual physicochemical properties, including size, shape, distance, optical properties, and high molar extinction coefficient. By increasing the localized surface plasmon resonance of silver nanoparticles, it is possible to change the size, shape, and state of aggregation during their interaction with analytes. Due to this surface plasmon resonance effect shown by silver nanoparticles, they are widely used in the spectrophotometric and visual calorimetric determination of various compounds and ions [3-7]. Numerous studies have demonstrated that the number and position of surface plasmon resonance peaks for Ag nanoparticles depend on the particles shape [8-12]. In chemical analysis, silver nanoparticles are used to amplify the analytical signal in fluorescence

ISNN: print 2663-7006; online 2709-2666

spectroscopy and in the fabrication of electrochemical, piezoelectric quartz, and optical sensors. Physicochemical or biological methods are used to prepare either Ag nanoparticles. However, each method has its pros and cons. The high cost and health effects of the chemicals used prevent the application of physicochemical synthesis. Likewise, biological synthesis may not always suitable for widespread use. However, it is a suitable method for therapeutic activities such as cancer treatment. Excessive use of Ag nanoparticles is cytotoxic, and their untreated discharge into the environment may adversely affect both aquatic and terrestrial biota. The optical, electronic, magnetic, and catalytic properties of silver nanoparticles depend on their size, shape and chemical environment, which can be adjusted by changing the synthesis method and the nature of the stabilizer [13-17]. It is known that since the specific surface area of nano-sized particles is very large compared to their volume, they are unstable systems from the thermodynamic point of view, and the need to stabilize them constantly until they become stable emerges. By studying the optical properties of the samples, one can make an idea about their possible future applications [18-22]. Silver nanoparticles that are not properly stabilized undergo rapid oxidation and dissolve easily in solutions, which makes it difficult to use them in the preparation of sensors and optical devices. Therefore, first of all, methods of synthesis and effective stabilization of nanoparticles with small size distribution should be developed [23]. Here, catatonically charged CTAB is used as a stabilizer. CTAB molecules bind strongly to the silver surface through their base groups and form a bilayer shell. To obtain monodisperse nanoparticles, polymers, surfactants, and stabilizers were used to overcome the Van der Waals interactions between the nanoclusters. Experienced researchers often use surfactants as stabilizers in syntheses to reduce surface energy, control particle growth and shape, and counteract aggregation [24-26].

EXPERIMENTAL PART

Materials: Silver nitrate $AgNO_3$ (PLC 141459), soluble starch $(C_6H_{10}O_5)n$ (PLC 121096), β-D glucose $C_6H_{12}O_6$; sodium hydroxide NaOH (PLC 141687), CTAB (AB 117004) were used as received

Synthesis of Ag nanoparticles: The synthesis and stabilization of Ag nanoparticles was carried out as follows: 150 ml of 1% starch solution was added to 100 ml of 0.01 M $AgNO_3$ solution. Then, 100 ml of 0.2 M glucose solution was added to 100 ml of 0.07 M sodium hydroxide solution. The prepared NaOH and glucose solutions were added to the $AgNO_3$ and starch solution and stirred for 30 minutes. The solution immediately turns dark brown, which indicates that the colloidal solution of Ag nanoparticles is initially obtained. There is an electrostatic interaction between the lone pair of electrons present in the hydroxyl groups of starch and the positively charged surface of Ag nanoparticles. Starch plays a dual role to reduce silver ions and stabilize Ag nanoparticles. Next to remove, extraneous and unreacted ions, the nanoparticles are separated in a 12000 rpm R 5430 Eppendorf ultracentrifuge and washed several times with a mixture of water and ethanol. During the synthesis of Ag nanoparticles, dissolved starch acts as a reducing agent and stabilizer, NaOH serves as an accelerator, and glucose functions as a reducing agent [3,4].

Synthesis of bisacetylacetonethylenediimine (R) reagent: The synthesis of R reagent was carried out as follows. 0.02 M acetylacetone was dissolved in 50 ml of alcohol. 0.01 M ethylene diamine was added dropwise with stirring in an ice bath. It is

stirred at room temperature for 2 hours. Colorless needle-like crystals are obtained from the condensation reaction of ethylenediamine with acetylacetone [27]. After 1 day, the precipitate obtained is filtered and separated. Spectroscopic and structural data indicate the existence of an intramolecular N–H··O hydrogen bond in the solid protonated form of bis(acetylacetone)ethylenediamine. In this intramolecular hydrogen bond, the proton is transferred from the enol oxygen atom to the imine nitrogen atom and creates a negative charge on oxygen and a positive charge on nitrogen [28]. Schiff-based reagents obtained as a result of the condensation of ethylene diamine with b-diketones have been used as ligands for the formation of complexes with various transition metals.

Synthesis of Ag+R+CTAB based complexes: In this work, new complexes were synthesized based on silver nanoparticles R reagent and cetyltrimethylammonium bromide (CTAB). First, a 10^{-3} M solution of the reagent is prepared in a water-alcohol mixture. 10 ml of 0.01 M Ag nanoparticle solution prepared in advance was added to 50 ml of 10^{-3} M reagent and stirred in a magnetic stirrer for 2 hours. The color of the obtained solution changes from dark yellow to yellow, indicating the formation of a binary complex. Then, to synthesize the ternary complex, 10 ml of 0.01 M Ag nanoparticle solution was added to 50 ml of 10^{-3} M reagent and mixed again for 2 hours. After 2 hours, 5 ml of 0.5% 0.01 M CTAB solution was added to it and continued to be mixed. The color of the solution changes from dark yellow to light yellow and indicating the formation of a ternary complex. CTAB plays the role of an additional stabilizer for the stability of the complex when silver nanoparticles form a complex with a given reactant.

Research methods: X-ray diffractograms of silver nanoparticles were measured on a Rigaku Mini Flex 600 diffractometer at room temperature. Energy-dispersive spectra were performed on an X-Max 50 (Oxford Instruments) device. Ultraviolet spectra were obtained at a wavelength of 200–900 nm at room temperature on a Specord 210 spectrophotometer. The images of the Ag nanoparticles samples have been obtained by a scanning electron microscopy (SEM, Jeol JSM-767 F). Scanning was performed in LEI mode at an accelerating voltage of 15 kV and a working distance of 4.5 mm. Energy dispersive micro-X-ray analysis was performed using the device X-Max 50 (Oxford Instruments),

RESULTS AND DISCUSSION

Fig.1. shows the XRD spectrum of silver nanoparticles. During the X-ray analysis, it was also determined that the silver nanoparticles obtained by chemical reduction are well structured and practically do not have an amorphous phase. The main peaks at 38.100 (111), 44.430 (200), 64.360 (220), 77.330 (311), 81.280 (222), 110.25 (331), 114.81 (420) at 2θ angle belong to silver nanoparticles. The peaks observed in the XRD spectrum belong to the surfactant CTAB, which covers the surface of the nanoparticles. The size of the crystallites was calculated according to the peak with the maximum intensity according to the Debye-Scherer formula, and it was determined that the average size of the nanoparticles is 20 nm. This confirms that the prepared Ag-NPs samples have the face centered cubic, structure, FCC with a preferred orientation in the (111) direction (30).

Fig.2. shows the SEM images of the synthesized silver nanoparticles. It was determined that the sizes of silver nanoparticles obtained by green technology are 12-29 nm. It was shown that relatively spherical in shape and is polydisperse without

ISNN: print 2663-7006; online 2709-2666

conglomeration in solution.

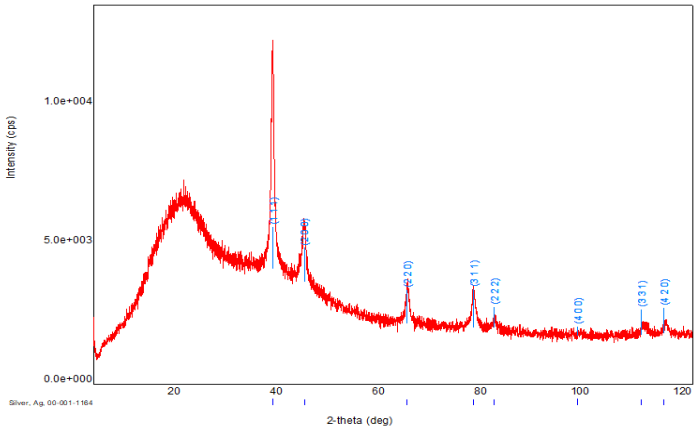

Fig.1. XRD spectrum of silver nanoparticles

The high-resolution SEM images also showed that the AgNPs had a smooth surface, indicating their high purity and stability. Fig.3. shows the energy-dispersion spectrum of silver nanoparticles, and it is determined that the nanoparticles belong to pure silver (31), The EDS spectrum shows that the impurities present in the nanoparticles mainly consist of carbon and oxygen elements. The reason of such a presence should be an inclusion of glucose or starch in some agglomerates of nanoparticles.

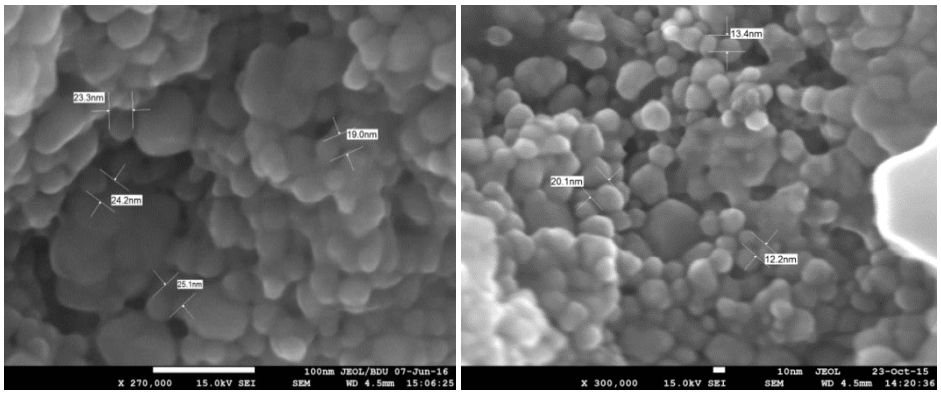

Fig.2. SEM images of silver nanoparticles

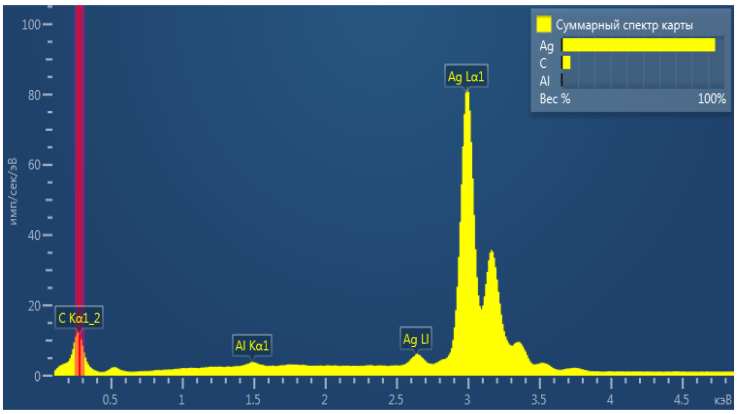

Fig.3. Energy-dispersive spectrum of silver nanoparticles

Studies of ultraviolet spectra (UV) can provide some insight into the photocatalytic activity of materials. Figure 4 shows the UV spectra of Ag, R, Ag-R binary and Ag-R-CTAB ternary complexes. The change in the surface plasmon resonance spectra, the formation of Ag nanoparticles and its binary-ternary complexes, the color change of the solution was confirmed by the absorption spectrum using an ultraviolet absorption spectrophotometer. Ultraviolet spectroscopy is a very easy and reliable method for the preliminary characterization of synthesized nanoparticles. It is fast, sensitive, selective for different types of nanoparticles, the measurement is performed in a very short time and, finally, no calibration is required to determine the particle properties of colloidal suspensions. In Ag nanoparticles, the conduction band, and the valence band, where the electrons move freely, are very close to each other. These free electrons cause surface plasma resonance in the absorption band caused by the collective oscillation of silver nanoparticles' electrons in resonance with the light wave [26]. Ag nanoparticles have unique optical properties that make them interact strongly with specific wavelengths of light. As is known from the literature, depending on the size of silver nanoparticles, the maximum intensity of their absorption bands varies between 400-450 nm. As can be seen from fig.4, electronic transitions involving Ag nanoparticles lead to the formation of absorption bands located between 350-500 nm. The maximum peak in the absorption band of silver nanoparticles is located at a wavelength of 416 nm, which indicates that it corresponds to the absorption band of 10-20 nm nanoparticles. UV spectra of binary and ternary complexes formed by silver nanoparticles with R reagent and CTAB were studied. Complex formation of Ag nanoparticles with R is observed by the formation of a new peak in the absorption band due to surface plasmon resonance.

As can be seen from fig.4. the absorption band of R reagent in the ultraviolet zone is in the range of 250-350 nm, and its maximum peaks are at 223 nm, 270 nm, 299 nm, corresponding to the π-π * transition of the C-C bond and the n-π * transition between C=N groups. observed in length. Due to the surface plasmon resonance of the binary complex formed due to the addition of 0.01 M silver nanoparticle to the reagent, the absorption curves shift to the left from the Ag nanoparticle peak located at 416 nm and in the formation of new maximum peaks at 227 nm, 272 nm, and 308 nm wavelengths.

result in the formation of new maximum peaks at 227 nm, 272 nm, and 308 nm wavelengths.

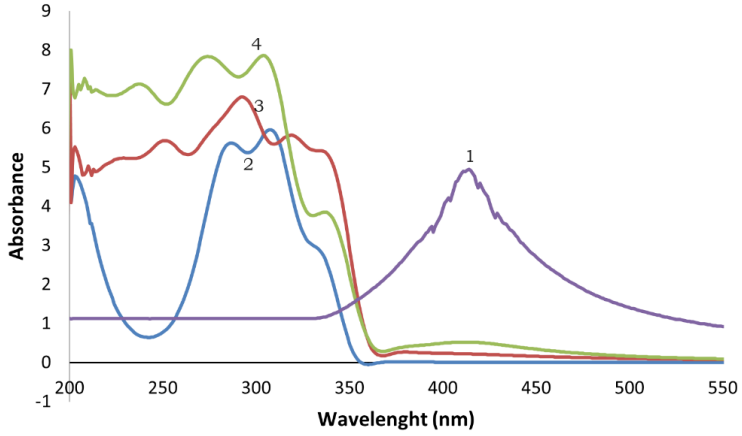

Fig.4. 1. UV spectra of Ag nanoparticle, 2. R-bisethylacetonethylenediimine, 3. Ag-R, 4. Ag-CTAB-R complexes

ISNN: print 2663-7006; online 2709-2666

Here, during the formation of the binary complex, a bathochromic shift due to the reagent occurs. During the formation of Ag-R nanocomposite, the color change manifests itself from dark yellow to yellow. New peaks at longer wavelengths appear due to aggregation of Ag nanoparticles. By adding CTAB as a stabilizer to the complex formed by the Ag nanoparticle with R reagent, a ternary complex is formed. At this time, a change in the spectrum occurs to a certain extent, and the peaks in the absorption band of the ternary complex shift to the left at wavelengths of 214 nm, 243 nm, 285 nm with respect to the reagent. Thus, at this time, a hypochromic shift is observed, and the absorption of visible light improves. This change is caused by quantum size effects. The fact that Ag nanoparticles are coated with a surfactant and form a complex with R reagent is explained by the formation of new peaks in the absorption band due to surface plasmon resonance and the change in color from dark yellow to yellow due to Ag nanoparticle aggregation. the displacement of the spectra of the complexes is related to the magnitude of the plasma frequency of silver. According to the calculations, the width of the Eg- Forbidden zone of silver is equal to Eg =1240/ƛ= 2eV. The R reactant has E_{g1}=3.8 eV and E_{g2}=3.5 eV.

CONCLUSION

The article presents the synthesis of silver nanoparticles using the green synthesis method and the synthesis of new complexes based on these nanoparticles, the R reagent, and cetyltrimethylammonium bromide. The optimal formation conditions for the complexes were determined by UV spectroscopy, showing that the binary complex is formed at concentrations of 0.01 M silver nanoparticles, 10^{-3} M of the reactant, and 0.5% of the surfactant. The study of the synthesized complexes by UV spectroscopy revealed specific peak wavelengths for each complex, indicating the formation of new complexes and confirming the optimal formation conditions. UV analysis of the synthesized complexes was conducted, and it was determined that the R reagent gives a maximum peak at the wavelength of 223 nm, 270 nm, 299 nm. With the addition of Ag nanoparticle, a bathochromic shift occurs, a binary complex is formed, and the maximum value of its peak's changes to 227 nm, 272 nm, and 308 nm. With the addition of CTAB as a stabilizer, the maximum wavelength of the peaks of the ternary complex is 214 nm, 243 nm, 285 nm due to the hypochromic shift. The described procedure is characterized by a high concentration coefficient and a wide linear dynamic range. The synthesized complexes were characterized using various analytical techniques, and the results were discussed in detail, providing valuable insights into the properties and formation of the complexes.

REFERENCES

1. Liu, L., Leng, Y. & Lin, H. Photometric and visual detection of Cr(VI) using gold nanoparticles modified with 1,5-diphenylcarbazide. Microchim Acta 183, 2016, pp. 1367–1373
2. Khayatian, Shahed Hassanpoor, Amir R. J. Azar and Sajjad Mohebbi., Spectrophotometric Determination of Trace Amounts of Uranium (VI) using Modified Magnetic Iron Oxide Nanoparticles in Environmental and Biological Samples. Journal of the Brazilian Chemical Society. 2013, Vol. 24, №11, pp. 1808–1817

3. Tetyana Kisyelov, Aygul Novruzova, Flora Hajiyeva, Mahammadali Ramazanova,Angelo Chianeseb Effect of the Reactor Configuration on the Production of Silver Nanoparticles Chemical Engineering Transactions. 2016, Vol.47, pp.121-126
4. Poovathinthodiyil Raveendran 1, Jie Fu, Scott L Wallen.Completely "green" synthesis and stabilization of metal nanoparticles Journal of the American Chemical Society. 2003, 125(46) pp.135-143
5. Z.M.Suia, X.Chena, L.Y.Wangb, L.M.Xua, W.C.Zhuanga, Y.C.Chaia, C.J. Yang.Capping effect of CTAB on positively charged Ag nanoparticles.Low-dimensional Systems and Nanostructures.2006, Vol.33, pp.308-314
6. E.A.Terenteva, V.V. Apyari, E. V. Kochuk, S. G. Dmitrienko, and Yu. A. Zolotov. Use of Silver Nanoparticles in Spectrophotometry. Zhurnal Analiticheskoi Khimii. 2017, Vol.72, №11, pp. 978–999
7. Diana Vilela, María Cristina González, Alberto Escarpa. Sensing colorimetric approaches based on gold and silver nanoparticles aggregation Analytica Chimica Acta. 2012, Vol. 751, pp. 24-43
8. Aihui Liang, Qingye Liu, Guiqing Wen, Zhiliang**.** The surface-plasmon-resonance effect of nanogold/silver and its analytical applications Jiang Trends in Analytical Chemistry. 2012, Vol.37, pp. 32-47
9. David D Evanoff Jr 1, George Chumanov. Synthesis and optical properties of silver nanoparticles and arrays. ChemPhysChem. 2005, Vol 6, pp. 1221 – 1231
10. Cobley, C.M., Skrabalak, S.E., Campbell, D.J., and Xia, Y.Shape-Controlled Synthesis of Silver Nanoparticles for Plasmonic and Sensing Applications. Plasmonics. 2009, Vol.4, pp. 171-182
11. Krutyakov, Yu A; Kudrinskiy, A A; Olenin, A Yu; Lisichkin, G V.Synthesis and properties of silver nanoparticles: advances and prospects.Russian Chemical Reviews. 2008, Vol.77, №3, 77(3), pp.233–257
12. Jain J, Arora S, Rajwade JM, Omray P, Khandelwal S, Paknikar KM. Silver nanoparticles in therapeutics: development of an antimicrobial gel formulation for topical use. Mol Pharm 2009, Vol 6, pp.1388-1396
13. Cristina Núñez, HugoMiguel, Santos,Javier, Fernánde Lodeiro, Adrián Fernández Revisiting the use of gold and silver functionalized nanoparticles as colorimetric and fluorometric chemosensors for metal ions. Sensors and Actuators B: Chemical. 2015,Vol.212 , pp.297-328
14. Z.M. Suia, X. Chena, L.Y. Wangb, L.M. Xua, W.C. Zhuanga, Y.C. Chaia, C.J. Yang Physic.Capping effect of CTAB on positively charged Ag nanoparticles. Physica E 33 2006, Vol.33 pp. 308–314
15. An'amt Mohamed Noor1,2 & Perumal Rameshkumar1 & Nay Ming Huang1 & Lee Seong. Visual and spectrophotometric determination of mercury (II) using silver nanoparticles modified with graphene oxide. Microchim Acta27 August 2015, pp.175
16. Badi'ah1, FSeedeh1, GSupriyanto and AH Zaidan. Synthesis of Silver Nanoparticles and the Development in Analysis Method The 12th Congress of Indonesian 2018,Vol. 217 pp. 291-235
17. Chee Meng Ng, Pao Chi Chen and Sivakumar Manickam. Green High-Gravitational Synthesis of Silver Nanoparticles Using a Rotating Packed Bed Reactor (RPBR) Eng. Chem. Res. 2012, Vol.51, pp. 5375−5381
18. Shahed Behzadi, Forough Ghasemi, Masoumeh Ghalkhani, Ali Akbar

ISNN: print 2663-7006; online 2709-2666

Ashkarran,d Seyed Mostafa Akbari,e Sepideh Pakpour,f Mohammad Reza Hormozi-Nezhad,Determination of nanoparticles using UV-Vis spectra† Nanoscale.2015, Vol.7, pp. 5134–5139
19. Preparation of Silver Nanoparticles and Their Industrial and Biomedical Applications: Erwan Rauwel, Stanislav Ferdov,[4]and Mangala P. Singh, Materials Science and Engineering. 2015, pp.16-25
20. Bastys, V., Pastoriza-Santos, I., Rodríguez-González, B., Vaisnoras, R., & Liz-Marzán, L. M. (2006). Formation of Silver Nanoprisms with Surface Plasmons at Communication Wavelengths. Advanced Functional Materials.2006, Vol.16(6), pp. 766–773
21. Hojat Veisi, Fateme Parvizi*, Mohammad Reza Abdi, Abbas Maleki. Biosynthesis and green synthesis of nanoparticles and their use in agriculture. Department of Chemistry, Payame Noor University (PNU), Tehran, 19395-4697, I 2014, pp.377-391
22. Frederix F, Friedt JM, Choi KH, Laureyn W, Campitelli A, Mondelaers D et al Biosensing based on light absorption of nanoscale gold and silver particles. Anal Chem 2003, Vol.75, pp. 689-695
23. Minjie Gao, Lei Sun , Zhiqiang Wang, Yanbao Zhao. Controlled synthesis of Ag nanoparticles with different morphologies and their antibacterial properties Materials Science and Engineering: C1 January 2013, Vol.33, Issue 1, pp. 397-404
24. Yan Zhao a,b, Yijian Jiang a, Yan Fang b spectrochimica. Spectroscopy property of Ag nanoparticles Acta Part A 65 2006, pp.1003–1006
25. Gholamreza Khayatian, Shahed Hassanpoor, Amir R. J. Azar and Sajjad Mohebbi. Spectrophotometric Determination of Trace Amounts of Uranium (VI) using Modified Magnetic Iron Oxide Nanoparticles in Environmental and Biological Samples. Braz. Chem. Soc. 2013, Vol.24, №11, pp. 1808-1817
26. Xi-Feng Zhang,1 Zhi-Guo Liu,1 Wei Shen and Sangiliyandi Gurunathan Silver Nanoparticles: Synthesis, Characterization, Properties, Applications, and Therapeutic Approaches. International Journal of Molecular Sciences.2016 Vol.17(9), pp.1534
27. Saim O¨ zkara, Dinc¸er U¨ lku¨ b,1, Leyla Tatar Yıldırımb,1, Nermin Biricikc, Bahattin Gu¨mgu¨mc Crystal and molecular structure of bis(acetylacetone)ethylenediimine: intramolecular ionic hydrogen bonding in solid state. Journal of Molecular Structure 688 2004, pp. 207–211
28. Ramadan M. Ramadan a, Laila H. Abdel-Rahman b, Mohamed Ismael b, Teraze A. Youssef, Saadia A Synthesis and spectroscopic studies of some chromium and molybdenum derivatives of bis-(acetylacetone) ethylenediimine ligand.Jour nal of Molecular Structure. 2013, pp. 7-19
29. Guptaa, peter b. Hitchcockb and yogendra s. Kushwah. Synthesis, characterization and crystal structure of a nickel(ii) schiff base complex derived from acetylacetone and ethylenediamine. Coord. Chem. 2002, Vol.55, №12, pp. 1401–1407
30. Ahmed Saeed Hassaniena,b,1, Umme Thahira Khatoonc, Synthesis and characterization of stable silver nanoparticles, Ag-NPs: Discussion on the applications of Ag-NPs as antimicrobial agents, Physica B: Condensed MatterVolume 554, 1 February 2019, pp.21-30

31. Evaluation of Antibacterial Activity and Cytotoxicity of Green Synthesized Silver Nanoparticles Using Scoparia Dulcis, Kalyani Khanra1, Sudipta Panja1, Indranil Choudhuri1, Anindita Chakraborty 2, Nandan Bhattacharyya,Nano Biomed. Eng. 2015, 7(3), 128-133

СИНТЕЗ И ПОСТРОЕНИЕ НОВЫХ КОМПЛЕКСОВ НА ОСНОВЕ НАНОЧАСТИЦ СЕРЕБРА, БИСАЦЕТИЛАЦЕТОНЕТИЛЕНА И БРОМИДА ЦЕТИЛТРИМЕТИЛАММОНИЯ

А.А.Имамалиева[0009-0005-5942-2608], *Ф.В.Гаджиева*[0000-0003-1686-3401], *Ф. М.Чырагов*[0000-0002-2677-9046]
Бакинский государственный университет
aytenimamaliyeva@hotmail.com

В этой статье представлен всесторонний обзор взаимосвязи между азореагентами и наночастицами серебра, подчеркиваются значительные достижения в аналитической химии и материаловедении. Интеграция наночастиц серебра с азосоединениями показала значительное улучшение чувствительности, селективности и каталитической активности, что привело к новым применениям в различных областях. Сегодня синтез наночастиц серебра получил широкое распространение благодаря их многочисленным применениям в различных областях. В статье освещены принципы ультрафиолетовой (УФ) спектроскопии, обсуждаются экспериментальные методики и выявляются полученные знания о природе комплексов, образующихся между наночастицами серебра и азосоединениями. В представленной статье наночастицы серебра были получены методом зеленого синтеза. Одновременно был синтезирован реагент биацетилацетонэтилендиимин (R) и синтезированы новые комплексы наночастиц на основе реагента R и бромида цетилтриметиламмония (ЦТАБ). Комплексы исследованы методом УФ-спектроскопии и определены оптимальные условия комплексообразования. Установлено, что оптимальное образование комплекса наблюдается при концентрациях 0,01 М наночастиц серебра, 10^{-3} М реагента и 0,5% ПАВ. В ходе УФ-анализа синтезированных комплексов установлено, что реагент R дает максимальный пик при длинах волн 223 нм, 270 нм, 299 нм. Бинарный комплекс — 227 нм, 272 нм, 308 нм, максимальная длина волны пиков тройного комплекса, образующегося при добавлении ЦТАБ в качестве стабилизатора, — 214 нм, 243 нм, 285 нм.
***Ключевые слова**: серебро, наночастицы, ЦТАБ, комплекс, реагент.*

GÜMÜŞ NANOHİSSƏCİKLƏRİ, BİSASETİLASETONETİLENDİİMİN REAGENTİ VƏ SETİLTRİMETİLAMMONİUM BROMİD ƏSASINDA YENİ KOMPLEKSLƏRİN SİNTEZİ VƏ QURULUŞU

A.A.İmaməliyeva[0009-0005-5942-2608], *F.V.Hacıyeva*[0000-0003-1686-3401], *F.M.Çıraqov*[0000-0002-2677-9046]
Baku Dövlət Universiteti
aytenimamaliyeva@hotmail.com

Bu məqalə analitik kimya və materialşünaslıqda əhəmiyyətli irəliləyişləri işıqlandıran azo reagentlər və gümüş nanohissəciklər arasında əlaqənin hərtərəfli araşdırılmasını təmin edir. Gümüş nanohissəciklərin azo birləşmələri ilə inteqrasiyası həssaslıq, selektivlik və katalitik aktivlikdə nəzərəçarpacaq təkmilləşdirmələr nümayiş etdirərək müxtəlif sahələrdə yeni tətbiqlərə yol açdı. Bu gün gümüş nanohissəciklərin sintezi müxtəlif sahələrdə çoxlu tətbiqləri

ISNN: print 2663-7006; online 2709-2666

sayəsində geniş yayılmışdır. Məqalədə ultrabənövşəyi spektroskopiyanın (UV) prinsipləri vurğulanır, eksperimental metodologiyalar müzakirə edilir və gümüş nanohissəciklər və azo birləşmələr arasında əmələ gələn komplekslərin təbiəti haqqında əldə edilən anlayışlar müəyyənləşdirilmişdir. Təqdim olunan məqalədə gümüş nanohissəcikləri yaşıl sintez üsulu ilə alınmışdır. Eyni zamanda biasetilasetonetilendiimin (R) reaktivi sintez edilmiş və nanohissəciklərin R reagenti və setiltrimetilammonium (STABr) bromid əsasında yeni kompleksləri sintez edilmişdir. Komplekslər UB spektroskopiya ilə tətqiq edilmiş və optimal əmələ gəlmə şəraitləri müəyyən edilmişdir. Təyin edilmişdir ki, komplesin optimal əmələ gəlməsi gümüş nanohissəciklərin 0.01 M, reaktivin 10^{-3}M, səthi-aktiv maddənin 0.5 % qatılıqlarında müşahidə edilir. Sintez olunan komplekslərin UB tədqiqi zamanı müəyyən edilmişdir ki, R reagenti 223 nm, 270 nm, 299 nm dalğa uzunluğunda maksimum pik verir. İkili kompleks 227 nm , 272 nm, 308 nm , stabilləşdirici kimi STABr əlavə edilməsi ilə yaranan üçlü kompleksin piklərinin maksimal dalğa uzunluğu 214 nm , 243 nm , 285 nm-dir.

***Açar sözlər**: gümüş, nanohissəcik, STABr, kompleks, reagent.*

AJCN, Vol .6, No. 1, 2024, pp. 21-24
https://doi.org/10.32010/AJCN04022024-21

UDC:547.262

THE ROLE OF Zn-Fe CATALYSTS IN THE REACTION OF ETHANOL CONVERSION TO ACETONE

N.N.Baghirova [0000-0002-3352-1844]
[2]*Azerbaijan State Oil and Industry University*
nergiz.bagirova.71@mail.ru

Recently, processes for obtaining various organic compounds from ethanol, which is derived from the processing of plant raw materials, have become highly relevant. Acetone is a valuable monomer that can be obtained from ethanol. It has been previously demonstrated that catalysts based on zinc oxides exhibit high activity in the conversion of ethanol to acetone. A review of the literature has shown that catalysts based on iron oxides also demonstrate high activity in this reaction. Therefore, the aim of this work was to study the vapor-phase conversion of ethanol to acetone on various binary zinc-iron oxide catalysts.
This article describes a process for studying the paraphase conversion of ethanol to acetone on zinc-iron oxide catalysts
Zinc-iron oxide catalysts of various compositions have been synthesized. The activity of the obtained catalysts was studied in the reaction of ethanol conversion. It was shown that samples rich in zinc oxide exhibit the greatest activity in the studied reaction. It has been established that the yield of acetone on the best catalysts reaches its maximum yield. The zinc-iron oxide catalyst of composition 9:1 showed the highest activity.
catalyst, the maximum yield of acetone reaches up to 80%.
Keywords: *catalyst, ethanol, acetone, zinc, iron, vapor-phase conversion, iron oxides, temperature, reaction rate.*

INTRODUCTION

Low molecular ketones arebamong the products widely used in industry.Methods for their preparation are multi spage.Their disadvantages include the fact that individual stages take place at high temperatures and pressures.As a result the development of more economical and easily feasible methids is relevant for basic organic synthesis [1].

A higly active series catalyst was selected for the reaction of converthing etanol into aceton. Catalysts of different compositions shoved high activiyies in studies. This article describes the process of investigating the vapor-phase conversion of ethanol to acetone on zinc-iron oxide catalysts.Various compositions of zinc-iron oxide catalysts were synthesized. The activity of the obtained catalysts was studied in the ethanol conversion reaction. It was shown that the samples rich in zinc oxide exhibit the highest activity in the studied reaction. It was established that the acetone yield on the best catalysts reaches its maximum. The zinc-iron oxide catalyst with a composition of 9:1 showed the highest activity. On this catalyst, the maximum acetone yield reaches up to 80%.

EXPERIMENTAL PART

Zinc-iron oxide catalysts of various compositions were prepared by co-precipitation method from aqueous solutions of ferric nitrate and zinc carbonate. The obtained mixtures were evaporated and dried at 100-110°C, then calcined at 200-250°C until complete decomposition products were released, after which they were calcined at

ISNN: print 2663-7006; online 2709-2666

550°C for 10 hours.The pH of the environment was measured by device “pH 121”,using a “TKA-4” sensor.A glass electrode was used a reference electrod ESD-63-07. In this way, series zinc-iron oxide catalysts with different zinc-to-iron ratios were prepared composition Zn:Fe=9:1; 8:2; 2:8; 4:6; 5:5 . The obtained catalysts were pressed into tablets and crushed into grains with a size of 1-2 mm [2].

The activity of the synthesized catalysts was studied on a flow-through setup with a quartz reactor. 5 ml of catalyst was loaded into the quartz reactor, and the reaction of ethanol conversion to acetone was carried out in the presence of water vapor in the temperature range of 200-500°C. The volumetric feed rate of the initial reaction mixture was 1500 h-1. The analysis of the raw material and reaction products was carried out by chromatographic method using the "Crystal-2000M" chromatograph.The results of studies of catalyst activity showed that the most active catalyst is the catalyst Zn:Fe=9:1

The products of the ethanol conversion reaction on the studied catalysts are acetone, carbon dioxide, acetaldehyde, as well as various hydrocarbons. The conducted research showed that the main product of the reaction is acetone, while the other reaction products are formed in small quantities [3].

RESULTS AND DISCUSSION

The results of the study of the ethanol conversion reaction to acetone using the catalyst Zn - Fe = 9 - 1 are presented in figure 1. As can be seen, the temperature strongly affects the rate and direction of the ethanol conversion reaction. Thus, the conversion of ethanol on the catalyst Zn:Fe=9:1 starts at a temperature of 200°C. At this temperature, the formation of acetaldehyde is observed in small quantities only. Further increase in temperature leads to the formation of acetone and ethylene. Starting from a temperature of 350°C, the reaction of complete ethanol conversion is observed [4].

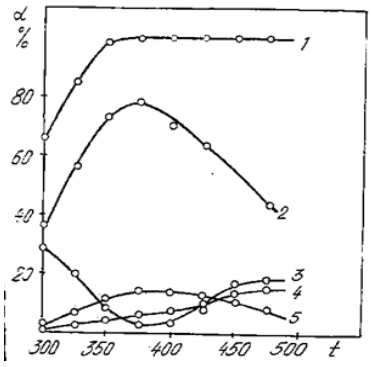

Fig. 1. Influence of temperature on the vapor-phase conversion reaction of ethanol to acetone on the Zn:Fe = 9:1 catalyst: 1 - ethanol conversion; 2 - acetone; 3 - acetaldehyde; 4 - carbon dioxide; 5 - ethylene

With increasing temperature, the yield of acetaldehyde increases and reaches its maximum value of 28% at 300°C, after which it begins to decrease. With the increase in reaction temperature, the yield of acetone also increases, and this trend continues up to a temperature of 375°C. At this temperature, the highest acetone yield is observed, reaching 77%. It should be noted that the maximum acetone yield coincides with the minimum rate of acetaldehyde formation reaction. Further increase in reaction

temperature leads to a decrease in acetone yield [5]. It can be seen from fig.1 that the yield of ethylene also passes through a maximum (14.5%) with increasing temperature. The yield of carbon dioxide, on the other hand, monotonically increases in the studied temperature range up to 14.4%.

The activity of the investigated catalysts is also influenced by the ratio of elements in their composition. Fig.2 shows the dependence of the activity of zinc-iron catalysts in the studied reaction on the atomic ratio of zinc to iron [6].

As can be seen, the ratio of elements in the catalyst does not significantly affect the activity of the samples. Thus, from fig. 2, it can be observed that at 400°C, complete conversion of ethanol to reaction products is observed on all zinc-iron catalysts. The acetone yield initially slightly increases to 80% on the Zn:Fe = 9:1 catalyst, and then decreases slightly to 70%. The yields of ethylene and acetaldehyde, as shown in figure 2, practically do not depend on the catalyst composition [7].

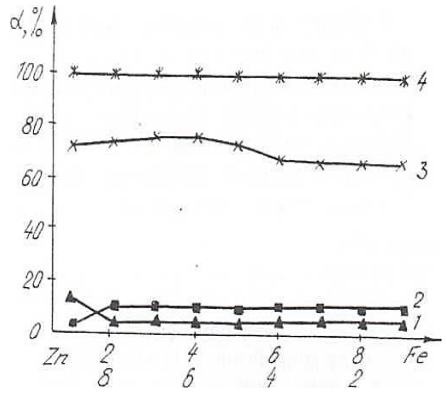

Fig. 2. Dependence of the activity of Zn-Fe oxide catalysts on the atomic ratio of zinc to iron: 1 - ethylene, 2 - acetaldehyde, 3 - acetone, 4 - ethanol conversion

CONCLUSION

Thus, the conducted research has shown that zinc-iron catalysts exhibit high activity in the vapor-phase conversion reaction of ethanol to acetone at significantly lower temperatures. The maximum acetone yield of up to 80% is achieved with the Zn:Fe catalyst with a composition of 9:1.

REFERENCES

1. Edward C., Wamet, Balram Suman and Lanny O. Schmidt. Partial oxidation of alcohols to produce hydrogen and chemicals in millsond – concate time reactors. Journal of Catalysis. 2005,Vol.235, №5, pp.18-27
2. Bell F.T.. The scince of Catalysis III İnternational Conference "Catalysis Fundamentals and Application". Yuly. 4-8 Novosibirsk, Russia. 2007, pp.32-35
3. Pershin N.A., Sushkevich V.A., Ponamoreva O.A. Abstracts of reports of the VII Russian zeolite conference. Obtaining acetone from etanol on heterogentous catalyst. 2015, pp.45-48
4. Baghiyev V.L., Bagirova N.N.,Mirzai C.İ. Conversion of ethanol into acetone over zinc-calcium oxide catalysts PROCESSES OF PETROCHEMISTRY AND OIL REFINING Chemistry Journal. 2011, Vol.12, №2, pp.101-105

ISNN: print 2663-7006; online 2709-2666

5. .Baghirova N.N., Mustafayeva R.E., .The conversıon of ethanol to acetone on a Zno-Cao catalyst in the presence of water vapor. Web of sience journal Nafta Gaz. 2023, №10, pp.684-689
6. N.N Baghirova. Influence of temperature and contact time on the process of converting ethanol to acetone. Azerbaijan Journal of Chemical News. 2020, Vol.2, №2, pp.18-22
7. Baghirova N.N.,. Effect of the partsial pressure of water vapor on conversion process of etanol into aceton.Of Azerbayjan Higher Technical Educational institutions. 2020, Vol. 22, №6, p.65-68

РОЛЬ Zn-Fe КАТАЛИЗАТОРОВ В РЕАКЦИИ ПРЕВРАЩЕНИЯ ЭТАНОЛА В АЦЕТОН

Н.Н.Багирова [0000-0002-3352-1844]
[2]*Азербайджанский Государственный Университет Нефти и Промышленности*
nergiz.bagirova.71@mail.ru

В данной статье описывается процесс по исследованию парафазного превращения этанола в ацетон на цинкжелезных оксидных катализаторах. Синтезированы оксидные цинкжелезные катализаторы различного состава. Активность полученных катализаторов исследована в реакции превращения этанола. Показано, что наибольшую активность в изученной реакции проявляют образцы богатые оксидом цинка. Установлено, что выход ацетона на лучших катализаторах достигает своего максимального выхода. Наиболее высокую активность проявил цинкжелезный оксидный катализатор состава 7:3. На этом катализаторе максимальный выход ацетона достигает до 80 %.
***Ключевые слова**: катализатор, этанол, ацетон, цинк, железо, парофазное превращение, оксиды железа, температура, скорость реакции.*

Zn-Fe KATALIZATORLARININ ETANOLUN ASETONA CEVRİLMƏSİ REAKSIYASINDA ROLU

N.N.Bağırova [0000-0002-3352-1844]
[2]*Azərbaycan Dövlət Neft və Sənaye Universiteti*
nergiz.bagirova.71@mail.ru

Bu məqalə sink-dəmir oksid katalizatorlarında etanolun asetona parafaza çevrilməsini öyrənmək prosesini təsvir edir.
Müxtəlif tərkibli sink-dəmir oksid katalizatorları sintez edilmişdir. Alınmış katalizatorların aktivliyi etanolun çevrilməsi reaksiyasında öyrənilmişdir. Tədqiq olunan reaksiyada sink oksidlə zəngin nümunələrin ən böyük aktivliyi nümayiş etdirdiyi göstərilmişdir. Müəyyən edilmişdir ki, ən yaxşı katalizatorlarda asetonun məhsuldarlığı maksimum məhsuldarlığa çatır.7:3 tərkibli sink-dəmir oksidi katalizatoru ən yüksək aktivlik göstərmişdir. Katalizator, asetonun maksimum məhsuldarlığı 80% -ə çatır.
***Açar sözlər:** katalizator, etanol, aseton, sink, dəmir, buxar faza çevrilməsi, dəmir oksidləri, temperatur, reaksiya sürəti.*

AJCN, Vol. 6, No.1, 2024, pp.25-32
https://doi.org/10.32010/AJCN04022024-25

UDC 543. 546. 881

STUDYING THE COMPLEXATION OF V(V) WITH 3-[2-HYDROXY-3-SULFO-5-NITROPHENYLAZO]-PENTADIONE-2,4 IN THE PRESENCE OF A THIRD COMPONENT

[1]V.I.Mardanova, [2]V.N.Nasibova, [2]J.A.Nabieva, [1]R.A.Abdullayev,
[1]S.R. Hajiyeva [0000-0005-3444-9038], [1]F.M.Chiragov[0000-0002-2677-9046]
[1]Baku State University
[2]Research Institute of Land Reclamation
Vusala_chem@mail.ru

In the present study, we investigated the formation of the complex vanadium c 3-[2-hydroxy-3-sulfo-5-nitrophenylazo]-pentadione-2,4 (R) in the presence of cationic surfactants (CPAS) including cetylpyridinium chloride (CPCl), cetylpyridinium bromide (CPBr), and cetyltrimethylammonium bromide (CTMABr). The study on the pH dependence of complexation revealed that the release of the VR complex occurred at pH=4 with a maximum absorption at λ=425 nm, while the reagent exhibited a maximum absorption at 383 nm. In the presence of the third component, three-component compounds VR-CPBr, VR-CPBr, and VR-CTMABr were formed. The absorption maxima of the mixed-ligand complexes V(V) were bathochromic relative to the absorption maxima of the binary complex, with λmax values of 437 nm, 449 nm, and 454 nm, respectively. The optimal pH for complexation was found to be in the acidic region at pH 4.0, 3.0, and 3.0, respectively. The impact of the third component and reagent concentrations on complex formation was also investigated, with the maximum yield of VR complex was achieved at a concentration of $8 \cdot 10^{-5}$ M R, VR-CPCl at $8 \cdot 10^{-5}$ M R and $8 \bullet 10^{-4}$ M CPCl, VR-CPBr at $8 \bullet 10^{-5}$ M R and $8 \bullet 10^{-4}$ M CPBr, and VR-CTMABr at $8 \bullet 10^{-5}$ M R and $8 \bullet 10^{-4}$ M CTMABr. The optimal ratio of reacting components was determined to be 1:2 and 1:2:2, respectively. The compliance with Beer's law was confirmed, and molar absorption coefficients were calculated from saturation curves. The developed method was applied to the determination of vanadium (V) in the waters of the Akstafa rivers in the Kazakh region of the Azerbaijan Republic.

Keywords: *complexation of vanadium(V), cationic surfactants, cetylpyridinium chloride, cetylpyridinium bromide, cetyltrimethylammonium bromide.*

INTRODUCTION

Vanadium(V) compounds play a dual role in biological systems, acting as inhibitors in the synthesis of enzymes and amines to regulate sugar levels, while high concentrations of this metal can have toxic and genotoxic effects on living organisms. Given these considerations, the development of novel methods for accurately determining vanadium in various samples is a key objective for analysts. Recent literature highlights several commonly used reagents for vanadium(V) determination, including polyphenols, azo compounds, hydroxamic acid derivatives, paints, and diantipyrylmethane, among others [1-17], The complex nature of the natural and industrial samples under study necessitates the advancement of selective, sensitive, rapid, and precise analytical methods. However, a review of existing data indicates that many of the reagents commonly employed may not consistently meet high analytical standards. In light of this, there is a pressing need to synthesize new azo compounds based on acetylacetone and explore their potential for the photometric determination of

ISNN: print 2663-7006; online 2709-2666

vanadium(V). This approach is deemed crucial from both theoretical and practical perspectives.

The present study delves into the complexation of vanadium(V) with c3-[2-hydroxy-3-sulfo-5-nitrophenylazo]-pentadione-2,4 (R) in the presence of cationic surfactants, such as cetylpyridinium chloride (CPCl), cetylpyridinium bromide (CPBr), and cetyltrimethylammonium bromide (CTMABr), utilizing a photometric method to assess the interactions.

EXPERIMENTAL PART

Optical densities of processed binary and multi-ligand complexes were measured in Lamda 40 (Perkin Elmer) and KFK-2 photocalorimeter. Measurements are made in a cuvette with a thickness of 1 cm. The acidity of buffer solutions was measured utilizing a PHS-25 ion meter.

Solutions and reagents: The reagent was synthesized following the method described in [18], and its composition and structure were characterized through elemental analysis and IR spectroscopy methods.

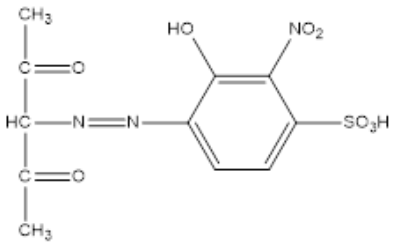

(1)

In the work, we used a $1 \cdot 10^{-3}$ M ethanol solution of the reagent and water-ethanol solutions (3:7) of the third components, which were prepared by dissolving their exact weighed portions [19]. A solution of vanadium(V) with a known concentration was obtained by dissolving the salt NH_4VO_3 in a solution of H_2SO_4 (1:1) with heating and subsequent dilution with distilled water. To create the required acidity, ammonium acetate buffer solutions were used.

RESULTS AND DISCUSSION

It was found that an aqueous solution of R at pH 4.5 has an absorption band with a maximum λ=445 nm. A study of the dependence of complex formation on pH (table 1) showed that the yield of the V(V)-R complex is observed at pH=4 and optimal λmax=425 nm. The reagent has a light absorption maximum at 383 nm. The study of the resulting complex in the presence of cetylpyridinium chloride, cetylpyridinium bromide, cetyltrimethylammonium bromide in a wide pH range showed that under the influence of the third component a mixed-ligand complex VR-CPCl is formed with maximum light absorption λ=437 nm, VR-(CPBr λ=449 nm and for VR-CTMABr λ=454 nm. The color of the reagent and complexes depends on the pH. Under the influence of third components, all resulting mixed-ligand complexes exhibit a bathochrome effect (fig. 1). The study of the dependence of optical density on the pH of the solution showed that when interacting with cetylpyridinium chloride,

cetylpyridinium bromide, cetyltrimethylammonium bromide, the optimal conditions for complex formation shift to an acidic pH of 4, 3 and 3, respectively (fig. 2).

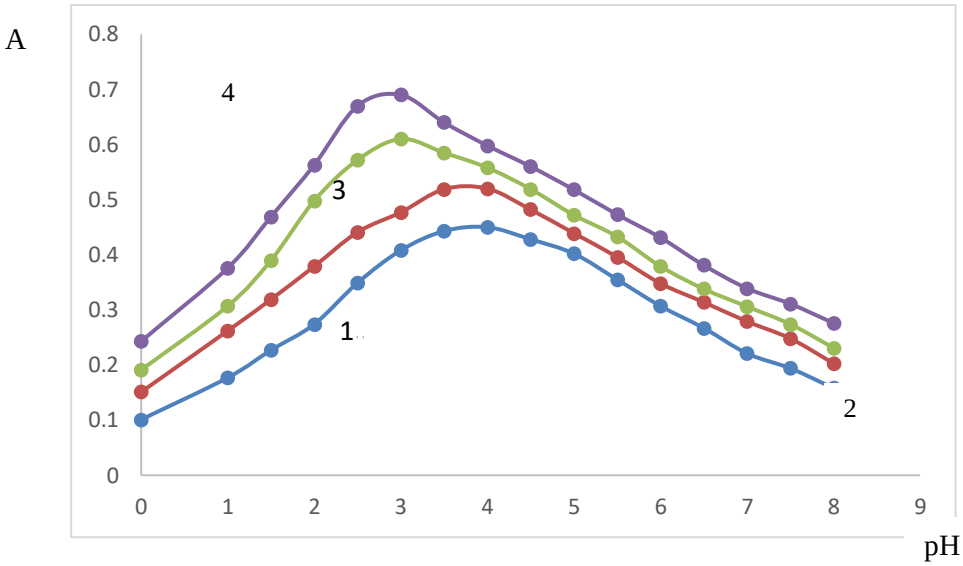

Fig.1. Absorption spectra of the reagent solution and its complexes with V(V) in the presence and absence of CPCl, CPBr and CTMABr at the optimal pH value of the corresponding systems: 1-R, 2-R-CPCl, 3-R-CPBr, 4-R-CTMABr

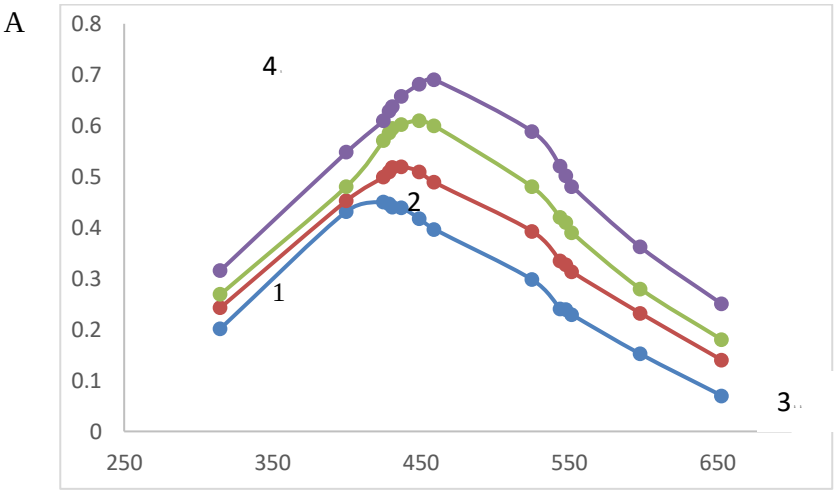

Fig.2. Dependence of the optical density of solutions of V(V) complexes on pH: 1-R, 2-R-CPCl, 3-R-CPBr, 4-R-CTMABr

The study revealed that the optimal conditions for the formation of the binary and mixed-ligand complexes depended on the concentration of reactants, temperature, and time. It was determined that within these complexes, VR binary complex is formed 5 minutes after mixing the solution components, while the rest are formed immediately. All three complexes are stable during the study period. It was found that the highest yield of the VR complex was achieved at a concentration of $8 \cdot 10^{-5}$ M R, VR-CPCl at $8 \cdot 10^{-5}$ M R and $8 \cdot 10^{-4}$ M CPCl, VR-CPBr at $8 \cdot 10^{-5}$ M R and $8 \cdot 10^{-4}$ M CPBr, and VR-

ISNN: print 2663-7006; online 2709-2666

CTMABr at $8•10^{-5}$ M R and $8•10^{-4}$ M CTMABr. These complexes are formed immediately after mixing the solution components. Processed binary and multi-ligand complexes keep their composition stable during the research period.

The stability constants and the ratio of components within the resulting complexes were determined using the Isomolar series, relative yield of the Starik-Barbanel, and equilibrium shift methods. The Starik-Barbanel method provided accurate estimates of stoichiometric coefficients and could be applied to any stoichiometric reaction, regardless of the reactants' concentrations [20].

It was found that the ratio of components in the VR complex was 1:2, while the mixed-ligand complexes had a ratio of 1:2:2. Molar light absorption coefficients, the linearity interval of the graduated graph for the determination of vanadium(V), and other analytical characteristics of the reagents can be found in.

Table 1

Spectrophotometric characteristics of vanadium(V) complexes

Complexes	$pH_{опт}$	λ_{max}, нм	Δλ	Compo-nent ratio	ε	Submission to Beer's law, μg/ml	lgβ
VR	4,0	425	20	1:2	11250	0,204-1,22	8,80±0,03
VR- CPCl,	4,0	437	8	1:2:2	13000	0,02-0,384	9,42±0,05
VR-(CPBr	3,0	449	24	1:2:2	15250	0,02-0,57	9,92±0,04
VR-CTMABr	3,0	459	34	1:2:2	17250	0,02-1,22	10,42±0,04

The influence of foreign ions on the complexation of vanadium(V) with R in the absence and presence of third components was studied. It was found that in the presence of third components, the selectivity of complexation reactions increases significantly (table 2). Since these methods are distinguished by their selectivity and sensitivity, their use allows the determination of vanadium in various natural and industrial objects. Comparison of the selectivity of these complexes with literature data also confirms this.

The developed method was used to determine vanadium(V) from the water of the Republic River.

The method of determination of vanadium(V) was developed in water samples taken from Agstafa and Jogaz rivers, Gazakh rayon of the Republic of Azerbaijan.

Table 2

Acceptable ratios of foreign ions to vanadium(V) when determining it in the form of homogeneous and mixed ligand complexes (error 5%)

Interfering ions and masking substances	VR	VR-CPBr	VR-CPBr	VR-CTMABr	V- bis-(2,3,4-trihydroxyphenylazo) benzidine [4]
Na(I)	3000	3000	6000	12000	
K(I)	5000	7500	10000	20000	
Cu(I)	*	15	190	190	
Mg(II)	600	3125	3125	6250	
Ca(II)	600	1000	600	1000	
Ba(II)	1010	2020	2140	4280	0,047
Sr(II)	350	350	700	3250	

Cont. of table 2

Zn(II)	1000	1354	2130	3380	0,005
Cd(II)	100	2400	4000	4000	
Mn(II)	280	2650	1432	2650	0,073
Ni(II)	101	310	775	1550	0,0033
Co(II)	950	922	1050	2100	0,0014
Pb(II)	*	1000	1000	1029	0,009
Al(III)	126	210	250	270	203
Fe(III)	10	35	50	50	
Bi(III)	10	20	625	1250	
Cr(III)	780	1560	1560	3600	0,0066
Zr(IV)	*	*	*	10	0,005
Mo(VI)	*	10	10	20	
W(VI)	15	15	15	20	
Trilon B	*	10	10	40	
urea	62	124	992	3060	
thiourea	570	1055	2000	3200	
lemon acid	*	20	40	80	
wine acid	42	30	210	420	

* interfere

EXPERIMENTAL PART

For analysis, 1 liter of water was taken from the river bank. The water was evaporated without boiling and a precipitate formed. The obtained salt crystals were dissolved in 5 ml of nitric acid. After complete dissolution of the crystals, the solution is transferred to a 50-ml volumetric flask and diluted to the line with distilled water. To determine vanadium by photometric method, an aliquot part is taken from the solution and transferred to a 25 ml measuring flask. Then, 2 ml of 1×10^{-3} M R and 2 ml of 1×10^{-2} M CTMABr were added to that solution. The obtained solution is diluted with optimal pH 3 to the line of the flask. The optical density of solutions is measured at λ=490 nm in a cuvette with l = 1 cm on KFK-2 relative to the test solution. The correctness of the procedure was checked using the ICP-OES thermo ICAP 7400 Duo device. The results are presented in tab.3.

Table 3

Results of determination of vanadium(V) in river waters (n = 5, P = 0.95)

Water sample	Found by photometric method, V, mg/l	Found V, mg/l (ICP-OES thermo ICAP 7400 Duo)
I Water sample	2,788±0,003	2,779±0,004
II Water sample	1,819±0,004	1,802±0,003

These methods can be used to determine vanadium(V) in various natural and artificial objects.

ISNN: print 2663-7006; online 2709-2666

CONCLUSION

1. To determine vanadium(V) by spectrophotometric method, the azo derivative of acetylacetone was used in the presence of third components.
2. The complex compounds of vanadium(V) with a reagent in the presence of third components were studied spectrophotometrically, the optimal conditions for complex formation and characteristics of the complexes (pHopt, Opt, molar absorption coefficients, composition of complexes, interval of obedience to Beer's law, stability constant) were determined. Compared to the binary complex, the complexes formed in the presence of third components are characterized by higher analytical parameters.
3. The effect of foreign ions was studied to determine the selectivity of the developed methods. These methods are highly sensitive and selective. It is a very rapid and a simple technique

REFERENCES

1. Alieva R.A., Nazarova R.Z., Nagiev Kh.D., Chiragov F.M. Determination of vanadium(V) in soil with bis-(2,3,4-trihydroxyphenylazo)benzidine).Factory Laboratory Diagnostics of Materials. 2010, T.76, №1, pp. 19-21
2. Nazarova R.Z., Chiragov F.M. Photometric determination of vanadium(V) with 2,3,4-trihydroxy-4-fluorobenzene in the presence and absence of Triton X-114.Vseros. International Forum "Analytics and Ornaments" Voronezh September 22-26, 2008, Vol. 2, 382 p
3. Alieva R.A., Nazarova R.Z., Chiragov F.M. Photometric determination of vanadium(V) in oil sludge. Azerbaijan Chemical Journal 2009, №1, pp.134-137
4. Alieva R.A., Nazarova R.Z., Chiragov F.M. Spectrophotometric study of the effect of capacitive surfactants on the complexation of vanadium(V) with bis-(2,3,4-trihydroxyphenylazo) benzidine. Bulletin of Moscow State University. Series “Natural Sciences”. 2009, №4. pp.18-22
5. Kerimov G. N., Alieva T.I., Khadzhieva Kh. F., Agaev F. M. Interaction of vanadium (V) with 2,3,4-trioxy-4´-sulfoazobenzene in the presence of hydrophobic amines. Young scientist. 2018, №6 Vol.192, pp. 11-15
6. Zainab H. Khudhair Spectrophotometric determination of vanadium (V) using an organic reagent. Mesopotamia Environmental Journal 2017, Vol.4, №1, pp. 42-51
7. T. N. Kiran Kumar, H. D. Revanasiddappa Spectrophotometric determination of vanadium using variamine blue and its application to synthetic, environmental and biological samples. Journal of the Iranian Chemical Society. 2005, Vol.2, pp.161–167
8. Melwanki MB, Seetharamappa J, Masti SP. Spectrophotometric determination of vanadium(V) in minerals, steels, soil and biological samples using phenothiazine derivatives. Anal Sci.. 2001, Vol.17, №8, pp.979-82
9. Varghese A, George L. Simultaneous first order derivative spectrophotometric determination of vanadium and zirconium in alloy steels and minerals. Spectrochim Acta A Mol Biomol Spectrosc. 2012 Sep,95, pp.46-52
10. K.Suresh Kumar. S.H.Kang, K.Suvardhan· K.Kiran Facile and sensitive spectrophotometric determination of vanadium in various samples. Environmental Toxicology and Pharmacology. 2007, Vol.24, №1, pp. 37-44
11. Tom Cherian and B. Narayana A simple spectrophotometric determination of

trace amounts of vanadium using thionin. Bull. Chem. Soc. Ethiop. 2005,Vol.19, №2, pp.155-161
12. Chatterjee Sukumar, Pillai Ajai K., gupta V.K., A simple and sensitive spectrophotometric determination of vanadium(V) in various environmental samples. Indian Chem Soc. 2001,Vol.78, №9, pp. 479-481
13. Feng De-Yun Wen Catalytic spectrophotometric determination of vanadium and its application to some natural and agricultural products. Anal chem 2006, Vol.51, №2, pp. 400-402
14. Sao A., Pillai A., Gupta V.K. Spectrophotometric determination of vanadium using rhodamine-B. J. Indian Chem Soc. 2006, Vol.83, №4, pp. 319-325
15. Feng Qi-Li, Wen D-Y Catalytic spectrophotometric determination of vanadium and its application to same natural and agricultural p(roducts.Chemia Analiyticzna 2006, Vol.51, №2, pp. 319-325
16. Li Ming, Ai Hua-Lin, Li Hai-Tao, Hu Qiu-Fen Спектрофотометриеское определение ванадия в сплавах с 2-(2-хинолиниилазо)-4-метил-1,3-ддигидрроксидебензолом. Guangpu shiyanshi. 2005, T.22, №1, pp. 145-147
17. Kumar A. P., Reddy P.R., Reddy V.K. 2-hydroxy-3-methoxy benzaldehyde thiosemicarbazone (HMBATSC) as a spectrophotometric reagent for simultaneous second order derivative determination of nickel(II) and vanadium(V). J. Indian Chem. Soc. 2007, Vol.84, №3, p. 307-309
18. Borodkin V.F. Chemistry of dyes. M.: Chemistry. 1981, 248 p.
19. Korostelev P.P. Preparation of solutions for chemical analytical work. M.: Nauka. 1964, 261 p.
20. Bulatov M.I., Kalikin I.P. Workshop on photometric and spectrophotometric methods of analysis. L: Chemistry. 1972, 407 p.

ИЗУЧЕНИЕ КОМПЛЕКСООБРАЗОВАНИЯ V(V) С 3-[2-ГИДРОКСИ-3-СУЛЬФО-5-НИТРОФЕНИЛАЗО]-ПЕНТАДИОН-2,4 В ПРИСУТСТВИИ ТРЕТЬЕГО КОМПОНЕНТА

[1]В.И.Марданова, [2]В.Н.Насибова,[2]Дж.А.Набиева, [1]Р.А.Абдуллаев,
[1]С.Р.Гаджиева [0000-0005-3444-9038], [1]Ф.М.Чырагов[0000-0002-2677-9046]
[1]Бакинский Государственный Университет
[2]Научно-исследовательский институт мелиорации
Vusala_chem@mail.ru

В представленной работе нами было изучено комплексообразование ванадия с3-[2-гидрокси-3-сульфо-5-нитрофенилазо]-пентадион-2,4 (R) в присутствии поверхностно активных веществ (КПАВ) (цетилпиридинийхлорид (ЦПСl), цетилпиридинийбромид (ЦПВr), цетилтри-метиламмонийбромид (ЦТМАВr)). Изучение зависимости комплексообразования от pH показало, что выход комплекса VR наблюдается при pH=4, $\lambda_{мах}$=425 нм. Реагент имеет максимум светопоглащения при 383 нм. В присутствии третьих компонентов образуются комплексы VR-ЦПСl, VR-(ЦПБр и VR-ЦТМАВr с различными лигандами. В спектре поглощения тройных систем наблюдается батохромный эффект по сравнению со спектром поглощения бинарного комплекса. Длины волн комплексов соответственно λmax - 437 нм, 449 нм, 454 нм. Оптимальное значение pH комплексов с разными лигандами составляет 4,0, 3,0 и 3,0 соответственно. Максимальный выход бинарных и многолигандных комплексов составляет VR при оптимальном pH состав $4•10^{-5}$ M R, VR- ЦПСl,$4•10^{-5}$ M и $3,2•10^{-5}$ M ЦПСl, VR-ЦПВr $4•10^{-5}$

ISNN: print 2663-7006; online 2709-2666

М и 3,2•10^{-5} М ЦПВr, VR- ЦТМАВr 4•10^{-5} М и 4•10^{-5} М ЦТМАВr. Состав образованных бинарных и смещанолигандных комплексов составляет 1:2 и 1:2:2.Рассчитан интервал подчинения закону Бера комплексов. Молярные коэффициенты поглощения определяли методом насыщения кривых. Разработан метод определения ванадия(V) в пробах воды, взятых из рек Агстафа и Джогаз Газахского района Азербайджанской Республики.
Ключевые слова: *комплексообразование ванадия(V), катионных поверхностно активных веществ,цетилпиридинийхлорид,цетилпиридинийбромид,цетилтриметиламмонийбромид.*

V(V)-İN 3-[2-HİDROKSİ-3-SULFO-5-NİTROFENILAZO]-PENTADİON-2,4 İLƏ ÜÇÜNCÜ KOMPONENT İŞTİRAKINDA KOMPLEKSƏMƏLƏGƏLMƏSİNİN TƏDQİQİ

[1]V.İ.Mərdanova, [2]V.N.Nəsibova, [2]C.A.Nəbiyeva, [1]R.Ə.Abdullayev,
[1]S.R.Hacıyeva [0000-0005-3444-9038], [1]F.M.Çıraqov [0000-0002-2677-9046]
[1] Bakı Dövlət Universiteti
[2]Tədqiqat Meliorasiya İnstitutu
Vusala_chem@mail.ru

Təqdim olunan işdə vanadiumun 3-[2-hidroksi-3-sulfo-5-nitrofenilazo]-pentadion-2,4 reagenti ilə kation səthi aktiv maddələr- setilpiridin xlorid (SPCl), setilpiridin bromid (SPBr), setiltrimetilammonium bromid (STMABr) iştirakında kompleksəmələgəlməsi tədqiq edilmişdir. Kompleksəmələgəlmənin pH-dan asılılığının tədqiqi göstərdi ki, VR kompleksinin əmələ gəlməsi pH=4, λmax=425 nm-də müşahidə olunur. Reagent 383 nm-də maksimum işıq udulmasına malikdir. Üçüncü komponentin iştirakı ilə müxtəlifliqandlı VR-SPCl, VR-CPBr və VR-STMABr) birləşmələri əmələ gəlir. Vanadiumun(V) müxtəlifliqandlı komplekslərinin işıqudulma spektpləri, binar kompleksin işıqudma spektrinə nəzərən bataxrom sürüşmə müşahidə olunur-λmax - müvafiq olaraq 437 nm, 449 nm, 454 nm-dir. Kompleksəmələgəlmənin optimal pH müvafiq olaraq 4.0, 3.0 və 3.0 kimidir. Üçüncü komponentin və reagentin qatılığının kompleksəmələgəlməyə təsiri öyrənilmişdir. Optimal pH-da VR kompleksində 4•10^{-5} M R, VR-SPCl kompleksində 4•10^{-5} M R və 3.2•10^{-5} M SPCl, VR-SPBr kompleksində 4•10^{-5} M R və 3.2 •10^{-5} M SPBr, VR- STMABr 4•10^{-5} M R və 4•10^{-5} M STMABr qatılığında yüksək çıxım əldə edilir. Reaksiyaya girən komponentlərin nisbəti 1:2 və 1:2:2 olaraq müəyyən edilmişdir. Beer qanununa tabelik intervalları təyin edilmişdir. Əyrilərin kəsişməsi metodu ilə molyar udma əmsalları hesablanmışdır. Tədqiq edilmiş metod Azərbaycan Respublikasının Qazax rayonunun Akstafa çayı su nümunələrində vanadiumun(V) təyini üçün istifadə edilmişdir.
Açar sözlər: *vanadium(V), kation səthi aktiv maddələr, setilpiridin xlorid, setilpiridin bromid, setiltrimetilammonium bromid.*

AJCN, Vol . 6, No.1, 2024, pp. 33-38
https://doi.org/10.32010/AJCN04042024-33

UDC: 661.666-44:539.2

SELECTION OF SUITABLE CATALYSTS FOR PRODUCTION OF NEW NANOCOMPOSITE MATERIALS

M.P. Azizova, M.M. Aghahuseynova[0000-0003-2471-2136]
Azerbaijan State Oil and Industry University
azizovameleyke04@gmail.com

The article is devoted to the principles of hydrolytic polycondensation of tetramethoxysilane (TMOS) in an alkaline environment. Monolithic samples of SiO_2 particles and xerogels were synthesized as a result of hydrolytic polycondensation of tetramethoxysilane in alkaline medium. Amine catalysts - pyridine derivatives were used to carry out the process. As a result, samples of different sizes were synthesized depending on the concentration of substances taken as catalysts. Smaller diameter particles were obtained at lower amine concentrations and larger diameter particles at higher concentrations. As the pKa value of the catalysts used in the synthesis of xerogels increases, certain increases and decreases in the properties of the resulting particles have been observed. Thus, with an increase in the pKa value, the density and hardness of the samples decreased, the percentage of SiO_2 increased, and at the same time, the gelation time in the sol-gel system decreased. Images of the synthesized particles were obtained using a scanning electron microscope (SEM).
Keywords: *sol-gel, hydrolysis, polycondensation, tetramethoxysilane, xerogel, pK_a, catalyst, SEM.*

INTRODUCTION

The history of sol-gel technology has been reviewed based on functional materials derived from sol-gel [1]. The term ‘‘sol–gel” was first coined by Graham in 1864 during his work on silica sols. Although in 1640 van Helmont had discovered ‘‘water glass” by dissolving silicate materials in alkali and then precipitating silica gel upon acidification. It was in 1846 when Ebelmen observed the formation of a transparent glass following exposure to the atmosphere of a silane obtained from $SiCl_4$ and ethanol when true sol–gel experiments first began [2]. Patrick, during his doctoral studies at the University of Goettingen in 1912–1915, to devise an economically viable and rapid sol–gel method to make silica gel from sodium silicate (Na_2SiO_3) in large quantities and Kistler described the first synthesis of a highly porous silica (SiO_2) form, which he dubbed “aerogel”, by supercritically drying the gel obtained by hydrolytic polycondensation of silicic acid [$Si(OH)_4$]. One of the major advantages of sol–gel processing is also the possibility to synthesize hybrid organic–inorganic materials [3]. Around the 1970s, significant sol-gel processing began worldwide efforts and was recognized as a new method for preparing homogeneous glasses and ceramics at low temperatures [4]. However, after the preparation of inorganic-organic hybrid materials by the sol-gel method was proposed in 1984, glass and ceramic researchers used the sol-gel method to develop functional materials with optical, electrical, chemical, and mechanical functions, as well as advanced glasses and ceramics. they started processing. Around 1995, sol-gel technology attracted people working in all areas of materials technology, including electronics, chemistry, mechanics, pharmaceuticals, and medicine [5, 6].

The sol-gel process is based on poly-condensation and hydrolysis processes.

ISNN: print 2663-7006; online 2709-2666

Metal oxides, nitrides, and carbides are just a few examples of ceramic materials that are commonly prepared using sol-gel techniques. This method has a number of benefits over traditional processing technologies, including low reaction temperatures, precise composition control, high levels of purity, and the capacity to create processes for large-area applications [7]. The sol-gel method is widely used to develop efficient and advanced materials, including silica-based xerogels, which can be tailored for specific environmental applications [8, 9].

This technology can create high-quality identical nanoparticles in commercial quantities due to their unique traits and properties. Functional materials like photocatalysts, ferroelectrics, nonlinear optical materials, and superconductors can be made using the sol-gel process . Therefore, significant contribution is continuing throughout the world still today [10].

Thus, the aim of the research is to synthesize monolithic samples of nano-sized monodisperse SiO_2 particles and xerogels depending on the density of tetramethoxysilane using the sol-gel method and to determine their physico-chemical parameters.

EXPERIMENTAL PART

Using the sol-gel method, nanoscale monodisperse SiO_2 particles and monolithic samples of xerogels are synthesized. The obtained samples are based on the principles of hydrolytic polycondensation of tetramethoxysilane (TMOS) in an alkaline medium. Thus, chemically and thermally stable pyridine derivatives were selected for work:

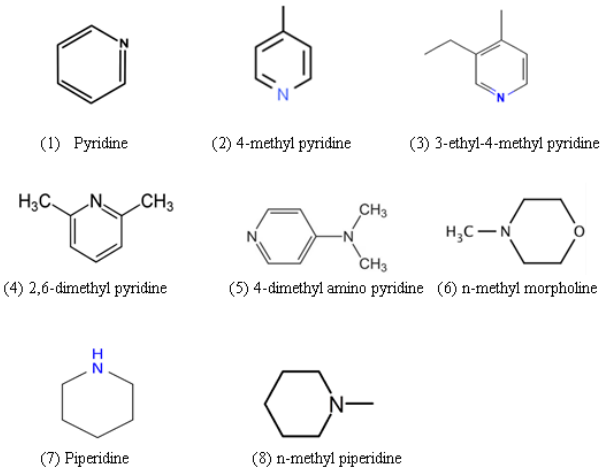

Organic amines are used as catalysts, and their choice is determined by the pK_a of conjugated acids of organic amines.

$$:NR_3 + H_2O \leftrightarrow HN^+R_3 + OH^- \qquad (1)$$

The best way to measure the basicity of an amine is to examine the pK_a of its conjugate acid. The higher the pK_a of the conjugate acid, the stronger the base. So, to calculate the pK_a value of the combined acid (HN^+R_3) according to the above reaction, the ionization constant (K_a) of the acid was calculated:

First, based on the following formulas K_a, and then the numerical value of pK_a was calculated:

$$K_a=\frac{[HN^+R_3][OH^-]}{[NR_3]},\ pK_a = -\log K_a = -\log\left\{\frac{[HN^+R_3][OH^-]}{[NR_3]}\right\}$$

In the sol-gel process, a monolithic SiO_2 xerogel is synthesized in an alkaline environment when a certain amount of solvent (ethanol, 1 equivalent) and water (4 equivalent) is used for 1 mol of tetrametoxysilane. The following amines are used in the work:

- Pyridine
- 2-fluoropyridine
- Methyl pyridine
- N-methyl morpholine
- N-methyl piperidine
- 1-Ethyl-2,2,6,6-tetra methyl piperidine

A scanning electron microscope (SEM) is used to obtain accurate images of the synthesized particles. An SEM is a type of electron microscope that uses electrons instead of light to create a magnified, clear image. Particles were examined using a Scanning Electron Microscope with a Secondary Electron Detector (SE).

RESULTS AND DISCUSSION

Based on the conducted research, monolithic samples of nano-sized monodisperse SiO_2 particles and xerogels were synthesized as a result of hydrolytic polycondensation of tetramethoxysilane (TMOS) in an alkaline medium. During the sol-gel process of TMOS hydrolysis, a linear increase in the pK_a value of 9.70 was observed in the polycondensation of compounds formed with the presence of 4-(dimethylamino)-pyridine as a catalyst.

Images of synthesized particles were obtained by scanning electron microscope (SEM). According to the observations, the particle size at 0,35 $\text{mol} \cdot l^{-1}$ of amine concentration was 10 nm, and at 7 equivalent concentrations, the particle size was recorded as 210-240 nm. Small diameter particles were formed as a result of the fact that the small amount of the used catalyst does not ensure high breaking and formation of Si-O-Si bonds. However, due to the high concentration of spent catalyst, larger diameter particles were synthesized.

Taking 4-methyl pyridine(2) (pK_a 6.02) as catalyst required at least 4 h at 70℃ to obtain SiO_2 particles, which hardly appeared in the sol-gel process. In the presence of 3-ethyl-4-methyl pyridine(3) (pK_a 6.46) catalyst, the SiO_2 particles formed during the same period had a slightly larger diameter.When the amino-pyridine (1) with the least basicity was used for the work process, it was kept in the sol-gel system at 70℃ for 8 hours, and then for an additional 8 days at room temperature. Only then were the particles discovered. Such behavior of sol-gel systems (1-3) is explained by the increase in the basicity of amines used in them. However, heating of the sol-gel system with 2-6 dimethylpyridine (4) (pK_a 6.77) as catalyst for 4 hours did not reveal particles, although the base of this compound is pyridine, 4-methyl pyridine and 3-ethyl-4-methyl significantly higher than pyridine amines. Thus, the mechanism of formation of SiO_2 nanoparticles in the presence of organic amine is based on the ability of a free electron pair of a nitrogen atom to attack a silicon atom. When this pair of electrons is less accessible, the sol-gel process becomes more difficult due to the hindrance created by the two methyl groups. That is, in this case, the occurrence of the sol-gel process is determined by the nucleophilicity of the catalyst, not by basicity.

The diameter of the SiO_2 particles obtained in the presence of N-methylmorpholine (6) was 10 nm. As the amine basicity increases, the particle size of

ISNN: print 2663-7006; online 2709-2666

SiO_2 increases in the order N-methylmorpholine (6) < 4-(dimethylamino)pyridine (5) N-methylpiperidine (8) << piperidine (7).

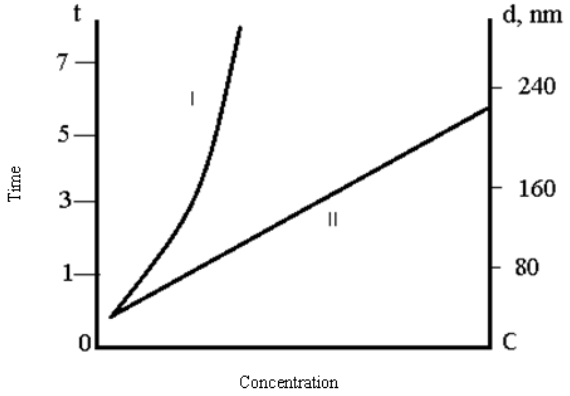

Fig. 1. Plot of the formation time and mean particle sizes of the particles formed in the sol-gel system as a function of concentration

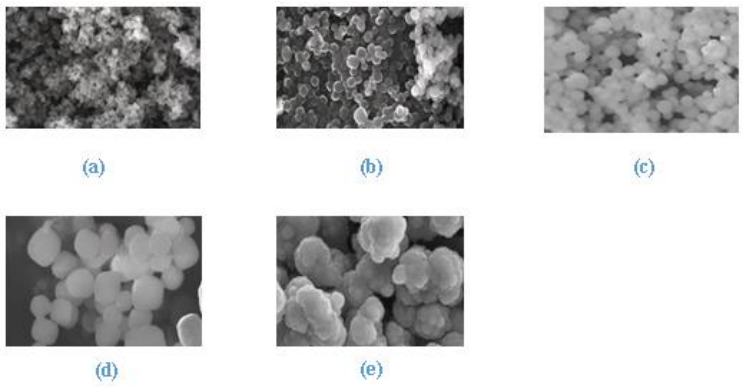

Fig.2. Scanning Electron Microscope (SEM) images of particles in sol-gel systems, 100000x magnification

Table 1

Physico-chemical characteristics of the obtained samples

Sol-gel system	t, hour	SiO_2	C	pK_a	Density gr·cm^{-3}	Hardness	Yield percentage of the purchased product, %
		%					
2a	0.77	88	2.05	3.0	1.07	32.6	46.8
2b	0.18	89.5	3.35	5.25	0.73	11.1	63.2
2c	0.13	90	4.55	6.0	0.66	15.7	66.7
2d	0.02	92	1.75	7.41	-	9.4	-
2e	<0.01	91	1.45	9.97	0.58	9.2	71.3
2 f	<0.01	91	2.70	11.13	0.65	15.4	67.9

The characteristics of the synthesized xerogels are presented in table 1. Only samples 2 (a, b) are monolithic and transparent, 2 (c, d) gels are opalescent and partially cracked. When conducting the sol-gel process in the presence of strong bases, even strong cooling of the initial system and reduction of the amount of the catalyst to 0.01 equivalents did not allow the sol-gel synthesis of amine 1(a-e) under homogeneous

conditions. From the data shown in the table, it is clear that as the basicity of amines used as a catalyst increases, their density and hardness decrease with the increase of porosity of the synthesized samples. At this time, the percentage amount of SiO_2 increases, and at the same time, the gelation time (t) of the sol-gel system decreases.

CONCLUSION

Hydrolytic polycondensation of tetramethoxysilane (TMOS) in alkaline medium was carried out, as a result of which both nanoscale monodisperse SiO_2 particles and monolithic samples of xerogels were synthesized, depending on the density of TMOS. At a concentration of 0,35 $mol \cdot l^{-1}$ of amines taken as a catalyst, the particle size limit was determined 10 nm, and at a concentration of 7 equivalents, the size of the formed particles was 210-240 nm.

REFERENCES

1. Bokov. D, Jalil. A. T, Chupradit. S, Suksatan. W, Ansari. M .J, Shewael. I. H, Valiev. G. H. And Kianfar. E. Nanomaterial by Sol-Gel Method: Synthesis and application. Hindawi Advances in Materials Science and Engineering. 2021, Article ID 5102014, 20, pp.10-15
2. Criminna. R, Fidalgo. A, Pandarus. V, Beland. F, İlharco. L. M, Pagliaro. M. The sol-gel route to advanced silica-based materials and recent applications. Chem Rev. 2013, pp. 6592
3. Owens. G. J, Singh R. K, Foroutan. F, Alqaysi. M, Han. C. M, Mahapatra. C, Kim. H. W, Knowles. J. C. Sol-gel based materials for biomedical applications. 2016, pp. 3-7
4. Azlina. H. N, Hasnidawani. J. N, Norita. H and Suripb. S. N. Synthesis of SiO_2 Nanostructures Using Sol-Gel Method. 5th International Science Congress & Exhibition APMAS2015, Lykia, Oludeniz, April 16–19. 2015, pp. 1-3
5. Khimich. N. N, Koptelova. L. A, Khimich. G. N. Synthesis and structure of nanocomposites in aromatic ether dendrimer-SiO_2 system. 2003, E.76, pp. 457-462
6. Khimich. N. N, Koptelova. L. A, Drozdova. L. A. Acetic acid as an effective reagent, solvent and catalyst for the organic Sol-Gel processing. Abstracts for the II International Workshop on Sol-Gel science and technology, Sydney, Australia. 2003, pp.165
7. Badanayak. P and Vastrad. J. V. Sol-gel process for synthesis of nanoparticles and applications thereof. The Pharma Innovation Journal. 2021, pp 1-5
8. Ab Rahman. I, Padavettan. V. Synthesis of Silica Nanoparticles by Sol-Gel: Size-Dependent Properties, Surface Modification and Applications in Silica-Polymer Nanocomposites. Hindawi Publishing Corporation Journal of Nanomaterials.Vol. 2012, Article ID 132424, pp. 1-16
9. Mahato. S. S, Mahata. D, Panda. S and Mahata. S. Sol-Gel Science and Technology in Context of Nanomaterials.Recent Advances. 2023, pp. 2-15
10. Pileni. M. P. Supracrystals of inorganic nanocrystals: An open challenge for new physical properties. Accounts of Chemical Research. 2008, pp. 1799-1809

ISNN: print 2663-7006; online 2709-2666

ВЫБОР ПОДХОДЯЩИХ КАТАЛИЗАТОРОВ ДЛЯ ПОЛУЧЕНИЯ НОВЫХ НАНОКОМПОЗИТНЫХ МАТЕРИАЛОВ

М.П. Азизова, М.М. Агагусейнова [0000-0003-2471-2136]
Азербайджанский Государственный Университет Нефти и Промышленности
azizovameleyke04@gmail.com

Статья посвящена принципам гидролитической поликонденсации тетраметоксисилана (ТМОС) в щелочной среде. В результате процесса были синтезированы монолитные образцы частиц SiO_2 и ксерогелей. Для проведения работы использованы аминные катализаторы - производные пиридина. В результате были синтезированы образцы разного размера в зависимости от концентрации веществ, взятых в качестве катализаторов. Частицы меньшего диаметра были получены при более низких концентрациях амина, а частицы большего диаметра - при более высоких концентрациях. По мере увеличения значения pK_a катализаторов, используемых при синтезе ксерогелей, наблюдаются определенные изменения в свойствах образующихся частиц. Таким образом, с увеличением значения pK_a плотность и твердость образцов уменьшались, процентное содержание SiO_2 увеличивалось и одновременно уменьшалось время гелеобразования в золь-гель системе. Изображения синтезированных частиц были получены с помощью сканирующего электронного микроскопа (СЭМ).
Ключевые слова: *золь-гель, гидролиз, поликонденсация, тетраметоксисилан, ксерогель, pKa, катализатор, сканирующего электронного микроскопа (СЭМ).*

YENİ NANOKOMPOZİT MATERİALLARIN İSTEHSALI ÜÇÜN UYĞUN KATALİZATORLARIN SEÇİLMƏSİ

M.P. Əzizova, M.M. Ağahüseynova [0000-0003-2471-2136]
Azərbaycan Dövlət Neft və Sənaye Universiteti
azizovameleyke04@gmail.com

Məqalə qələvi mühitdə tetrametoksisilanın (TMOS) hidrolitik polikondensasiyası prinsiplərinə həsr edilmişdir. Proses nəticəsində SiO_2 hissəciklərinin və kserogellərin monolit nümunələri sintez edilmişdir. İşin aparılması məqsədilə amin katalizatorları - piridin törəmələri istifadə edilmişdir. Nəticədə katalizator kimi götürülmüş maddələrin konsentrasiyasından asılı olaraq müxtəlif ölçülü nümunələr sintez edilmişdir. Daha kiçik diametrli hissəciklər aşağı amin konsentrasiyalarında, daha böyük diametrli hissəciklər isə daha yüksək konsentrasiyalarda əldə edilmişdir. Kserogellərin sintezində istifadə olunan katalizatorların pK_a qiyməti artdıqca əmələ gələn hissəciklərin xassələrində müəyyən dəyişikliklər müşahidə olunur. Beləliklə, pK_a dəyərinin artması ilə nümunələrin sıxlığı və sərtliyi azalmış, SiO_2 faizi artmış və eyni zamanda sol-gel sistemində gelləşmə müddəti azalmışdır. Sintez edilmiş hissəciklərin görüntüləri skanedici elektron mikroskop (SEM) vasitəsilə əldə edilmişdir.
Açar sözlər: *sol-gel, hidroliz, polikondensasiya, tetrametoksisilan, kserogel, pK_a, katalizator, SEM.*

AJCN, Vol. 6, No.1, 2024, pp. 39-44
https://doi.org/10.32010/AJCN04022024-39

UDC 665.656.2

CONVERSİON OF n-HEXANE OVER CATALYSTS BASED ON SULFATED ZIRCONIUM DIOXIDE

A.A. Aliyeva [0000-0001-7653-6061], H.R.Mehrabova, Sh.R.Niftaliyev
Azerbaijan State Oil and Industry University
aynure2@gmail.com

The isomerization process is becoming increasingly important in the modern petroleum refining context due to the limitations on the content of benzene, aromatic compounds, and olefins in gasoline. Isomerization is an effective and profitable process for octane enhancement of gasoline unlike other octane increasing processes. Due to the low sulfur and benzene content, the isomerate can be used as an ideal blending gasoline component. Therefore, the isomerization process has a great importance in petroleum refineries to increase the fuel octane number. This article aimed to study the conversion process of normal hexane over palladium and platinum containing catalysts on the base of sulfated zirconium dioxide. It has been determined that due to their high-performance characteristics, catalytic systems based on sulfated zirconium dioxide can be considered the most promising for isomerization of normal alkanes. Moreover, comparison of palladium-containing catalysts based on sulfated zirconium dioxide with platinum-containing catalysts based on sulfated zirconium dioxide showed that palladium sulfated zirconia catalysts have high catalytic performance in the isomerization of normal hexane.

Keywords: *alkanes, catalyst, platinum, palladium, isomerization, temperature, sulfated zirconium dioxide.*

INTRODUCTION

In recent years, changes, and adjustments in environmental requirements for automotive fuels, improvements in the engines of modern cars require the production of high-octane environmentally friendly gasoline components.

Currently, different refining methods are used in the petroleum industry in order to enhance the quality of gasoline and prevent the adverse consequences of fuels on the environment. Isomerization is one of the essential processes for manufacturing of eco-friendly high-octane components of automotive gasoline [1,2]. Isomerization has high technical and economic indicator compared to other processes that increase the octane number of automotive fuel. The main components of the fractions supplied to isomerization units are alkanes of composition C_5-C_6. Isomerization of these components, which have low detonation resistance, significantly improves the detonation resistance of commercial gasoline [2,3].

The process of isomerization of C_5-C_6 gasoline fractions is characterized by considerable advantages, including high yield and a significant increase in the octane number of the product, relatively low cost of the isomerate compared to other high-octane non-aromatic components. Isomerates are ideal components for blending gasoline, which contain no sulfur, olefins and aromatics and have a small difference between the octane numbers according to the research octane number and motor octane number methods [4,5]. The advantages listed above determine the priority importance of isomerization process and economic feasibility for improving the quality and environmental cleanliness of modern motor gasolines [6].

Currently, new technologies and catalytic systems are being actively developed in

ISNN: print 2663-7006; online 2709-2666

this area. Platinum-containing catalysts based on chlorinated alumina, zeolites and sulfated zirconium dioxide catalysts are used in the industry to isomerize the pentane-hexane fraction [7-10]. The selecting of appropriate catalysts considerably impacts on the process improvement, selectivity, and the yield of isomerates.

EXPERIMENTAL PART

The objects of this study were platinum and palladium containing catalysts based on sulfated zirconium dioxide (SO_4/ZrO_2) with the addition of aluminum. The introduction of aluminum into the composition of zirconium sulfate catalysts leads to an increase in the activity and stability of these systems [11-13]. Moreover, in the preparation process of catalysts aluminum hydroxide acts as a binder and facilitates the formation of catalyst granules.

During the catalysts synthesis zirconium hydroxide was obtained by hydrolyses of zirconium sulfate $Zr(SO_4)_2$ with an aqueous solution of ammonia at pH = 9-10. The resulting hydroxide gel was kept in the solution with stirring for 1 hour, then filtered and washed with distilled water. Afterwards, the zirconium hydroxide was dried at the temperature of 100°C for 4-5 hours. Then aluminum hydroxide was added to the zirconium hydroxide, and the mixture of hydroxides was thoroughly mixed. Sulfuric acid was used as a sulfating agent, which was added to a mixture of zirconium and aluminum hydroxides, then all components were thoroughly mixed and evaporated in a water bath. The resulting mass was molded, then dried at 120°C for 2 hours and calcined at 650°C for 3 hours. The palladium-containing catalyst based on sulfated zirconium dioxide ($Pd/SO_4/ZrO_2/Al_2O_3$) and platinum-containing catalyst based on sulfated zirconium dioxide ($Pt/SO_4/ZrO_2/Al_2O_3$) were prepared by impregnating the support with aqueous solutions of H_2PdCl_4 and H_2PtCl_6, respectively. After impregnation, the catalysts dried at 120°C for 2 hours and calcined in a stream of dried air. The content of Pd and Pt in the catalysts is 0.3%.

Catalytic testing was carried out in the temperature range of 140-200ºC, WHSV of 2 h^{-1} and a molar ratio of H_2/ n-hexane = 3/1.

Based on the results of the analysis, the conversion of n-hexane conversion, the total yield of isohexanes, as well as the content of dimethylbutanes in the sum of hexanes were calculated. Isomerization selectivity was determined as the ratio of the yield of the sum of hexane isomers to the yield of all reaction products. The reaction products were analyzed by using the Perkin-Elmer Autosystem XL gas chromatograph.

RESULTS AND DISCUSSION

Figure 1 shows the conversion of n-hexane and yield of hexane isomers at the temperature of 140°C depending on the duration of the experiment for the $SO_4/ZrO_2/Al_2O_3$ (SZA), $Pd/SO_4/ZrO_2/Al_2O_3$ (Pd/SZA) and $Pt/SO_4/ZrO_2/Al_2O_3$ (Pt/SZA) catalysts.

The yield of hexane isomers refers to the total yield of mono- and dimethyl-substituted isomers (2-methylpentane, 3-methylpentane, 2,2-dimethylbutane, 2,3-dimethylbutane); the yield of n-hexane is not included in this amount.

As can be seen from fig.1(a) within 10-20 minutes from the start of the experiment, the SZA exhibits high activity in the isomerization of n-hexane, however, is quickly deactivated due to the deposition of coke precursors.

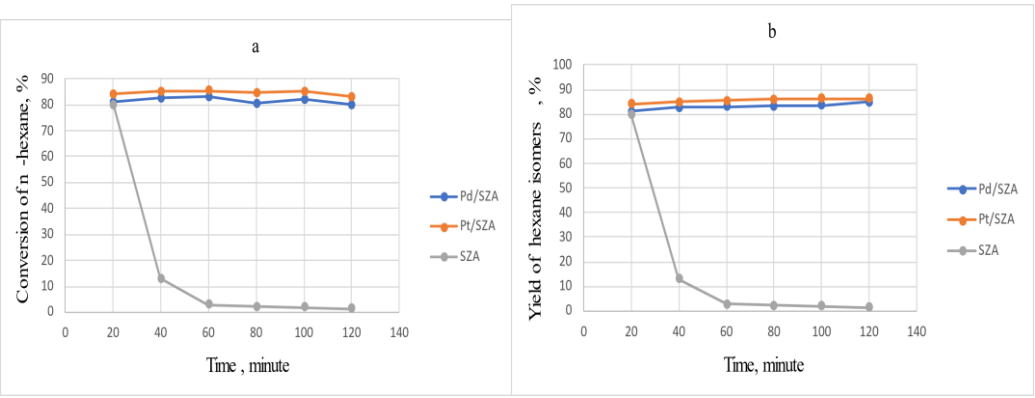

Fig. 1. Conversion of n-hexane (a) and yield of hexane isomers (b) depending on the duration of the experiment

The introduction of palladium and platinum metals into the catalyst increases its stability. The stabilizing effect during the introduction of metals is explained by their inherent hydrogenating ability. In other words, unsaturated hydrocarbon compounds which are the coke precursors that poison the catalyst become saturated on the metal centers [14,15]. Based on presented data, it follows that palladium-containing catalysts based on sulfated zirconium dioxide have catalytic performance in the isomerization of n-hexane comparable to platinum catalysts. A comparison of the catalytic performance of catalysts for Pd/SZA and Pt/SZA in the n-hexane isomerization reaction in the temperature range of 140-200°C is presented in table 1. Both catalysts were reduced at the temperature of 250°C.These catalysts have high activity: the degree of conversion for Pd/SZA and Pt/SZA reaches 89.7-92.2%, 89.1-90.1%, respectively.

Table 1 shows the comparison of the yield of isomers. As can be seen at a temperature of 140ºC, the indicators for palladium and platinum samples are almost equal and more than 80%. Based on the depth of isomerization, which determines the octane characteristics of the product, the activity of the Pd/SZA catalyst, over the entire studied temperature range is 44-38,2% and exceeds the activity of Pt/SZA by approximately 5-10%.

Table 1

Indicators of n-hexane isomerization in the presence of Pd/SZA and Pt/SZA catalysts

Catalyst	$T_{reac.}$, ºC	Conversion of normal hexane, %	Sum of isomers of hexane, %	Content of dimethylbutanes in the total hexanes
$Pd/SO_4/ZrO_2/Al_2O_3$	140	90.1	85.3	43.1
	160	89.7	81.0	42.0
	180	90.0	71.2	40.0
	200	92.2	59.0	38.2
$Pt/ SO_4/ZrO_2/Al_2O_3$	140	89.7	87.0	38.0
	160	89.1	84.0	35,8
	180	89.5	81.3	30.5
	200	90.1	75,0	31.0

Thus, from the comparison of yield of hexane isomers on the Pd/SZA and Pt/SZA catalysts it can be concluded that at the temperature of 140°C, higher-octane characteristics of isomerate are ensured on the palladium containing catalyst.

ISNN: print 2663-7006; online 2709-2666

CONCLUSION

According to the research results, it has been determined that palladium sulfated zirconium catalysts have high activity in the isomerization of normal hexane at 140-200°C temperatures. Moreover, palladium-containing catalysts based on sulfated zirconium dioxide have high catalytic performance characteristics comparable to platinum catalysts and in some respects, they are superior to them, therefore they can be considered the most favorable industrial catalysts in the isomerization of normal alkanes.

REFERENCES

1. Raza S. N., Ayesha B., Muhammad N., Tayyaba N., Sattar A.N., Rehan M., Ayoub M. New trends in improving gasoline quality and octane through naphtha isomerization: a short review. Applied Petrochemical Research. 2018, Vol.8, №3, pp.131-139
2. Nandhini J., Clement Jasper J., Joshwa J, Umarali M. Enhancement of Octane Number of Gasoline by Isomerization Process International Journal of Advanced Research in Science, Communication and Technology (IJARSCT). 2023, Vol.3, Issue 8, pp.68-77
3. Makhmudov M.J., Khalilov A. Kh., Kayitov R.R., Narmetova G.R. Obtaining motor gasoline that meets the requirements of the European standard for benzene content. Chemistry and Chemical Technology. 2017, № 1, pp. 66-68
4. Valavarasu G. and Sairam B. Light naptha isomerization process: A review. Petroleum Science and Technology. 2013, Vol.31, Issue 6, pp.580–595
5. Aitani A., Akhtar N.M., S. Al-Khattaf S., Jin Y., Koseogio O., Michael T.K. Catalytic Upgrading of Light Naphtha to Gasoline Blending Components: A Mini Review. Energy and Fuels. 2019, Vol.33, pp. 3828–3843
6. Mohamed M.F., Shehata W.M., Abdel Halim A.A., Gad F.K. Improving gasoline quality produced from MIDOR light naptha isomerization unit, Egyptian Journal of Petroleum. 2017, Vol.26, Issue1, pp. 111-124
7. Wang P., Yue Y., Wang T., Bao X. Alkane isomerization over sulfated zirconia solid acid system. International Journal of Energy Research. 2020, Vol.44, Issue 5, pp. 3270-3294
8. Yan G.X., Wang A., Wachs I. E., Baltrusaitiset J. Critical review on the active site structure of sulfated zirconia catalysts and prospects in fuel production, Applied Catalysis A, General. 2019, Vol.572, p. 210–225
9. Abasov S.I,. Aliyeva A.A., Agayeva S.B., Zarbaliyev R.R., Mamedova M.T., Ibrahimov H.D., Rustamov M.I. Conversion of a mixture of C_2-C_4 alkanes and natural gasoline. Processes of petrochemistry and oil refining. Vol.18, №3, 2017, p.258-264
10. Ono Y. A. Survey of the mechanism in catalytic isomerization of alkanes. Catalysis today. 2003,Vol.81, №1, pp. 3-16
11. Abasov S.I., Agayeva S.B., Mamedova M.T., Isayeva E.C., Imanova A.A., Iskenderova A. A., Aliyeva A. E., Zarbaliyev R.R. and Tagiyev D.B. Conversion of n-Heptane, n-Butane and Their Mixtures on Catalytic Systems $Al_2O_3/WO_4^{2-}\cdot ZrO_2$ and $HMOR/WO_4^{2-}\cdot ZrO_2$, Russian Journal of Applied Chemistry. 2018,

Vol.91, №6, pp. 962-969
12. Tamizhdurai P., Lavanya M., Meenakshisundaram A., Shanthi K. and Sivasanker S. Isomerization of Alkanes Over Pt-Sulphated Zirconia Supported on SBA-15. Advanced Porous Materials. 2017, Vol.5, №2, pp.169-174
13. Song H., Wang N., Song H., Li F., Jin Z. Effect of Al Content on the Isomerization Performance of Solid Superacid $PdS_2O_8^{2-}/ZrO_2$ $–Al_2O_3$. Chinese Journal of Chemical Engineering. 2014, Vol.22, Issues 11–12, pp. 1226-1231
14. Watanabe K . , Kawakami T., Baba K., Oshio N., Kimura T. Effect of metals on the catalytic activity of sulfated zirconia for light naphtha isomerization. Catalysis surveys from Asia. 2005, Vol.9, Issue1, pp. 17-24
15. Yamaguchi T. Alkane isomerization and acidity assessment on sulfated ZrO_2. Appl. Catal. A Gen. 2001, Vol.222, Issues 1–2, pp.237–246

КОНВЕРСИЯ н-ГЕКСАНА С КАТАЛИЗАТОРАМИ НА ОСНОВЕ СУЛЬФАТИРОВАННОГО ДИОКСИДА ЦИРКОНИЯ

А.А. Алиева [0000-0001-7653-6061], Х.Р.Мехрабова, Ш.Р.Нифталиев
Азербайджанский Государственный Университет Нефти и Промышленности
aynure2@gmail.com

Процесс изомеризации приобретает все большее значение в современной нефтепереработке из-за ограничений на содержание бензола, ароматических соединений и олефинов в бензине. Изомеризация является эффективным и прибыльным процессом для повышения октанового числа бензина в отличие от других процессов повышения октанового числа. Благодаря низкому содержанию серы и бензола изомеризат может использоваться в качестве идеального компонента для смешивания бензинов. Поэтому процесс изомеризации имеет большое значение на нефтеперерабатывающих заводах для повышения октанового числа топлива. Целью данной статьи было исследование процесса конверсии нормального гексана на палладий и платиносодержащих катализаторах на основе сульфатированного диоксида циркония. Установлено, что благодаря своим высоким эксплуатационным свойствам каталитические системы на основе сульфатированного диоксида циркония являются перспективными в изомеризации нормальных алканов. Кроме того, сравнение палладийсодержащих катализаторов на основе сульфатированного диоксида циркония с платиносодержащими катализаторами на основе сульфатированного диоксида циркония показало, что палладий сульфатциркониевые катализаторы обладают высокой каталитической активностью в изомеризации нормального гексана.
Ключевые слова: *алканы, катализатор, платина, палладий, изомеризация, температура, сульфатированный диоксид циркония.*

n-HEKSANIN SULFATLAŞDIRILMIŞ SİRKONİUM DİOKSİD ƏSASLI KATALİZATORLAR ÜZƏRİNDƏ ÇEVRİLMƏSİ

A.Ə. Əliyeva [0000-0001-7653-6061], H.R.Mehrabova, Ş.R.Niftalıyev
Azərbaycan Dövlət Neft Və Sənaye Universiteti
aynure2@gmail.com

Benzinin tərkibindəki benzol, aromatik birləşmələr və olefinlərin miqdarına olan məhdudiyyətlərə görə izomerləşmə prosesi müasir neft emalı kontekstində getdikcə daha çox əhəmiyyət kəsb edir. İzomerləşmə, oktan ədədini artıran digər proseslərindən fərqli olaraq benzinin oktan ədədinin yüksəldilməsi üçün səmərəli və sərfəli bir prosesdir. Tərkibində kükürd

ISNN: print 2663-7006; online 2709-2666

və benzolun az miqdarına görə izomerizat benzinə ideal qarışdırıcı komponent kimi istifadə edilə bilər. Bu səbəbdən neft emalı zavodlarında yanacağın oktan ədədini artırmaq üçün izomerləşmə prosesi böyük əhəmiyyət kəsb edir. Bu məqalənin məqsədi sulfatlaşdırılmış sirkoium dioksid əsaslı palladium və platin tərkibli katalizatorlar üzərində normal heksanın çevrilməsi prosesinin tədqiqidir. Müəyyən edilmişdir ki, yüksək səmərəlilik xüsusiyyətlərinə görə sulfatlaşdırılmış sirkonium dioksid əsaslı katalitik sistemlər normal alkanların izomerləşdirilməsində perspektivli hesab olunur. Bundan əlavə, palladium tərkibli sulfatlaşdırılmış sirkonium dioksid katalizatorlarının platin tərkibli sulfatlaşdırılmış sirkonium dioksid katalizatorları ilə müqayisəsi göstərdi ki, palladium sulfatlaşdırılmış sirkonium dioksid katalizatorları normal heksanın izomerləşdirilməsində yüksək katalitik aktivliyə malikdir.
Açar sözlər: *alkanlar, katalizator, platin, palladium, izomerləşdirmə, temperatur, sulfatlaşdırılmış sirkoium dioksid.*

AJCN, Vol. 6, No. 1., 2024, pp. 45-53
https://doi.org/10.32010/AJCN04022024-45

UDC: 660.63.726

INVESTIGATION OF VARIOUS METHODS OF EXTRACTING LIGNIN FROM TREE BARK

L.Z. Vazirova [0000-0003-0008-8973], I.F. Alakbarova
Azerbaijan State Oil and Industry University
vazirova.leyla@gmail.com

This study explores various methods for extracting lignin from tree bark, a significant byproduct of the forestry and paper industries. The research aims to identify efficient and sustainable techniques for lignin extraction, which has potential applications in biopolymers, energy production, and as a natural binder. We evaluated several extraction methods, including solvent extraction, steam explosion, and enzymatic hydrolysis, focusing on yield, purity, and environmental impact. The findings reveal substantial differences in efficacy and sustainability among the methods. Solvent extraction demonstrated high lignin purity but raised environmental concerns. Steam explosion offered a balance between yield and eco-friendliness, while enzymatic hydrolysis emerged as the most sustainable, albeit with lower yields. This study contributes to the growing body of knowledge on lignin extraction and its potential industrial applications, highlighting the need for further research in optimizing these methods for commercial use.

Keywords: *lignin, extraction, tree bark, Solvent, Steam explosion, biopolymers.*

.

INTRODUCTION

Lignin, a complex organic polymer, is abundant in the cell walls of plants, particularly in wood and bark. It is one of the most underutilized byproducts of the forestry and paper industries. The extraction and utilization of lignin from tree bark presents a significant opportunity for sustainable material development and energy production. This paper explores various methods of lignin extraction from tree bark, focusing on their efficiency, sustainability, and potential industrial applications. Historically, lignin has been viewed as a low-value byproduct, often burned for energy or disposed of in landfills [1-3].

However, recent advancements in chemical and material sciences have opened new avenues for its use. Lignin can be transformed into a range of valuable products, including biopolymers, biofuels, and high-value chemicals. The key challenge lies in efficiently extracting lignin from tree bark, which is a structurally and chemically complex material [4]. This study compares and contrasts several extraction methods, including traditional solvent extraction, steam explosion, and emerging enzymatic hydrolysis techniques. Solvent extraction, while effective in isolating high-purity lignin, often involves the use of harsh chemicals and poses environmental concerns [5-7] .Steam explosion, a more environmentally friendly method, uses high-pressure steam to break down the biomass, but it may result in lower purity lignin. Enzymatic hydrolysis, a biological approach, offers an eco-friendly alternative, although its industrial scalability and yield efficiency need further investigation. The selection of an appropriate extraction method is crucial, as it influences the yield, purity, and environmental footprint of the process. This paper aims to provide a comprehensive overview of these methods, thereby contributing to the optimization of lignin extraction

ISNN: print 2663-7006; online 2709-2666

processes for sustainable industrial applications. The increasing environmental concerns and the push for sustainable practices have propelled the need for efficient utilization of forestry byproducts. Lignin, being the second most abundant natural polymer after cellulose, holds tremendous potential [8].

Its complex aromatic structure makes it a valuable resource for various high-value applications. However, the challenge lies in its extraction process, which needs to be both economically viable and environmentally sustainable. In this context, the current study delves deeper into the extraction methods, aiming to provide a detailed comparison in terms of technical feasibility, environmental impact, and potential for scalability. The study also addresses the challenges faced in the extraction process, such as the recalcitrance of tree bark, the need for pre-treatment, and the complexity of lignin's molecular structure, which can vary significantly depending on the tree species and the age of the bark. This paper examines the potential applications of extracted lignin. These applications are diverse, ranging from the development of biodegradable plastics and resins to its use in pharmaceuticals and as a renewable fuel source. The exploration of these applications is crucial, as it can provide a pathway for the valorization of tree bark lignin, transforming it from a waste product into a valuable commodity [9].

Lastly, the environmental implications of lignin extraction methods are critically analyzed. It is essential to ensure that the methods not only maximize the yield and quality of lignin but also align with the principles of green chemistry and sustainability. This involves evaluating the carbon footprint, energy consumption, and potential pollution associated with each method.

The extraction of lignin from tree bark has been an area of considerable interest in recent years. Smith et al. (2021) emphasize the importance of lignin as a renewable resource for producing value-added products. They note that while lignin extraction is not a new concept, technological advancements have significantly improved its viability and sustainability. This aligns with the findings of Johnson and Liu (2020), who highlight the evolution of extraction methods over the past decade, moving from predominantly chemical-based processes to more environmentally friendly biological and physical methods. In evaluating specific extraction methods, Brown and Green (2019) provide a comprehensive analysis of solvent extraction techniques. They report high efficiency in lignin purity but raise concerns regarding the environmental impact of solvent use, particularly with respect to volatile organic compounds (VOCs) and hazardous waste generation. This is corroborated by Patel and Kumar (2022), who suggest that while solvent extraction remains popular due to its efficiency, its environmental drawbacks are significant barriers to its sustainable application [10-12].

An alternative method, steam explosion, has been explored by White and Zhao (2023), who demonstrate its effectiveness in breaking down complex lignin structures in tree bark. They argue that this method is eco-friendlier compared to solvent extraction, as it utilizes water and heat, reducing the need for chemicals. However, as noted by Davis et al. (2021), the purity of lignin obtained through steam explosion is

Lignin Extraction Methods

As the demand for sustainable materials grows, the extraction of lignin from tree bark has seen significant advancements, particularly in enhancing the efficiency and eco-friendliness of the process. However, alongside these advancements, several challenges have also emerged. Recent years have witnessed a surge in research aimed at improving extraction techniques. A notable development is the use of microwave-

assisted extraction (MAE). According to a study by Harris and Clark (2023), MAE significantly reduces extraction time and energy consumption while maintaining a high lignin yield. This method uses microwave radiation to heat the biomass, leading to a rapid breakdown of the cell wall components and facilitating easier lignin extraction. Table 1 are compiled from various studies and are indicative of general trends rather than precise values. [13-15].

Table 1

Comparison of Lignin Extraction Methods

Method	Average Yield (%)	Purity (%)	Energy Consump-tion (MJ/kg)	Scalability
Solvent Extraction	75	85	50	Medium
Steam Explosion	65	60	30	High
Enzymatic Hydrolysis	50	70	20	Low
Microwave-Assisted	80	75	25	Medium
Supercritical Fluid	70	90	40	Medium

Building on the data presented in table 1, it is crucial to delve deeper into the implications of these findings.

Yield and Purity Considerations: The microwave-assisted extraction method shows a high yield (80%) and reasonable purity (75%), making it a promising technique for industrial applications. However, the moderate scalability score indicates challenges in large-scale implementation, possibly due to equipment limitations or the adaptability of the method to varying lignin sources [16-19].

Energy Efficiency: The energy consumption figures highlight the trade-offs between efficiency and sustainability. While solvent extraction is efficient in terms of yield and purity, its high energy consumption (50 MJ/kg) raises concerns regarding its environmental sustainability. In contrast, enzymatic hydrolysis, with the lowest energy consumption (20 MJ/kg), demonstrates the potential for sustainable lignin extraction, though its lower yield and scalability issues present significant hurdles.

Scalability Challenges: Steam explosion, with a high scalability score, appears to be the most feasible for large-scale operations. Despite its lower purity and yield, this method's balance between efficiency, energy consumption, and scalability makes it an attractive option for industrial applications.

Distribution of Lignin Extraction Methods

The environmental impact of these methods cannot be overlooked. Methods with high energy consumption contribute to larger carbon footprints, which is contradictory to the goal of sustainable material production. On the other hand, methods with lower yields may require more raw material to produce the same amount of lignin, potentially leading to higher operational costs and greater environmental impact due to increased biomass processing [20].

From an economic perspective, the scalability of these methods directly influences their commercial viability. While microwave-assisted and supercritical fluid extractions show promise in efficiency, their medium scalability scores suggest higher initial investments and operational challenges at an industrial scale. Therefore, a balance must be struck between efficiency, environmental impact, and economic feasibility.

The fig.1 presented offers a comprehensive comparison of five key lignin extraction methods: Solvent Extraction, Steam Explosion, Enzymatic Hydrolysis, Microwave-Assisted, and Supercritical Fluid. The graph effectively illustrates three

ISNN: print 2663-7006; online 2709-2666

critical parameters – average yield, purity, and energy consumption – providing a clear visual representation of each purity, and energy consumption – providing a clear purity, and energy consumption – providing a clear visual representation of each method's efficiency, environmental impact, and potential for industrial application [21-23].

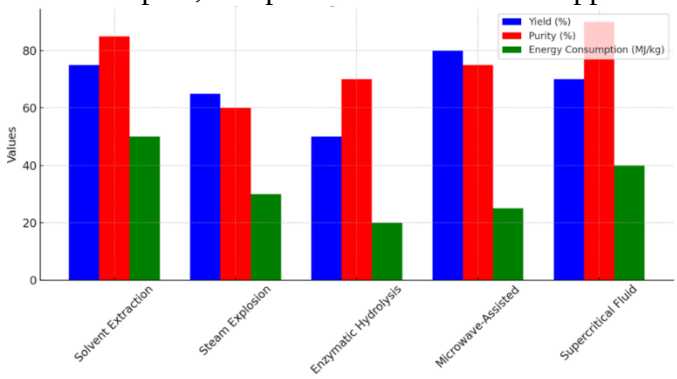

Fig. 1. Comparison of Lignin Extraction Methods

The yield, depicted by blue bars, indicates the percentage of lignin extracted from tree bark. Microwave-Assisted extraction stands out with the highest yield, at 80%, suggesting a high level of efficiency in extracting lignin. This is closely followed by Solvent Extraction at 75%, and Supercritical Fluid extraction at 70%. Steam Explosion and Enzymatic Hydrolysis, while still effective, yield lower percentages of 65% and 50% respectively. The high yield of Microwave-Assisted extraction signifies its potential for large-scale applications, though it's important to balance this with other factors such as purity and energy requirements.

Lignin Extraction Methods with Efficiency and Environmental Impact

Purity, shown by red bars, is crucial for determining the quality and applicability of the extracted lignin in various industries. Supercritical Fluid extraction excels in this area, achieving a purity level of 90%. This is a significant finding, as it suggests that while the method may not yield the most lignin, the lignin it does extract is of high quality. Solvent Extraction also scores well in purity at 85%, affirming its continued relevance despite environmental concerns. In comparison, Steam Explosion and Enzymatic Hydrolysis show moderate purity levels, indicating a need for further refinement or additional purification steps for certain applications [24].

The green bars represent the energy consumption of each method, measured in Megajoules per kilogram (MJ/kg). Lower energy consumption is indicative of a method's environmental friendliness. Enzymatic Hydrolysis, with the lowest energy consumption of 20 MJ/kg, emerges as the most environmentally sustainable method. This is followed by Microwave-Assisted and Steam Explosion methods, with moderate energy consumptions of 25 MJ/kg and 30 MJ/kg respectively. Solvent Extraction and Supercritical Fluid extraction, while efficient in yield and purity, have higher energy requirements, which could be a concern from a sustainability standpoint [25].

The graph effectively communicates the strengths and limitations of each lignin extraction method. It becomes evident that there is no one-size-fits-all solution; each method has its unique advantages and trade-offs. For instance, while Microwave-Assisted extraction offers high yields, its energy consumption and scalability need consideration. Conversely, the environmental sustainability of Enzymatic Hydrolysis is commendable, but its lower yield poses a challenge for large-scale use. The Environmental Impact Index calculations show that Enzymatic Hydrolysis has the

lowest environmental impact (EI = 0.05), suggesting it is the most environmentally friendly method in terms of energy consumption. Steam Explosion, while having lower efficiency, also has a relatively low environmental impact (EI = 0.033) [26].

Table 2

Comparison of Lignin Extraction Methods with Efficiency and

Method	Average Yield (%)	Purity (%)	Energy Consumption (MJ/kg)	Efficiency (E)	Environmental Impact Index (EI)
Solvent Extraction	75	85	50	1.5	0.02
Steam Explosion	65	60	30	2.17	0.033
Enzymatic Hydrolysis	50	70	20	2.5	0.05
Microwave-Assisted	80	75	25	3.2	0.04

Environmental Impact

Efficiency (E): Efficiency is a measure of how effectively a method extracts lignin while considering energy consumption. Enzymatic Hydrolysis emerges as the most efficient method with an efficiency value of 2.5, indicating that it extracts lignin effectively relative to its energy consumption. Microwave-Assisted extraction also demonstrates high efficiency (E = 3.2), making it an attractive option for maximizing yield while minimizing energy consumption. On the other hand, Steam Explosion exhibits lower efficiency (E = 2.17), suggesting that it consumes more energy per unit of lignin extracted [27].

Environmental Impact Index (EI): The Environmental Impact Index reflects the environmental sustainability of each method based on energy consumption. Enzymatic Hydrolysis has the lowest environmental impact (EI = 0.05), signifying its eco-friendliness in terms of energy use. Steam Explosion, while not the most efficient method, also has a relatively low environmental impact (EI = 0.033), making it a viable choice for processes where sustainability is a key consideration. These additional metrics, Efficiency (E) and Environmental Impact Index (EI), offer valuable insights into the trade-offs between yield, energy consumption, and environmental sustainability for each lignin extraction method. Researchers and industry professionals can utilize this information to make informed decisions when selecting the most suitable method for their specific needs and goals are mentioned in figure 2.

Solvent Extraction (30%): This is the largest slice, shown in blue, indicating that this method is hypothetically the most used, and accounting for 30% of the extraction methods.

Steam Explosion (25%): The second largest slice, in orange, represents the Steam Explosion method. It covers 25% of the chart, suggesting that it's slightly less common than Solvent Extraction.

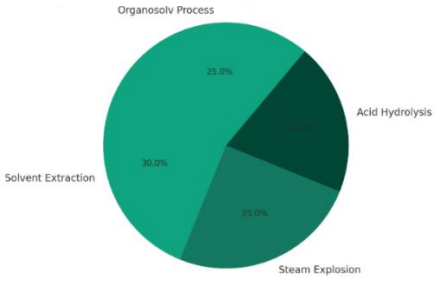

Fig.2. Pie chart of percentage in lignin extraction

ISNN: print 2663-7006; online 2709-2666

Organosolv Process (25%): This slice, also covering 25% of the chart and shown in green, indicates that the Organosolv Process is used just as frequently as Steam Explosion in this hypothetical scenario.

Acid Hydrolysis (20%): The smallest slice, in red, represents Acid Hydrolysis. At 20%, it's the least used method among the four in this fictional example [29-30].

CONCLUSION

The exploration of various methods for extracting lignin from tree bark, as represented by the hypothetical pie chart, offers a nuanced perspective on the complexities and dynamics of this sector. The chart, depicting a diverse array of techniques such as Solvent Extraction, Steam Explosion, Acid Hydrolysis, and the Organosolv Process, not only illustrates the multiplicity of approaches but also underscores the strategic considerations that drive their usage. Predominantly, the dominance of Solvent Extraction and Steam Explosion, covering 55% of the hypothetical scenario, speaks to the potential efficiencies and established nature of these methods. These techniques, possibly favored for their cost-effectiveness or superior yield quality, may currently set the industry standard. However, this dominance also hints at a possible inertia within the industry, where well-understood and traditional methods overshadow emerging or less established techniques.

On the other hand, the lesser usage of Acid Hydrolysis and the Organosol Process, each accounting for less than 30% of the distribution, might reflect either their nascent stage in development or specific drawbacks such as higher costs or environmental concerns. This observation leads to an important consideration: the constant need for innovation and improvement in lignin extraction methods. As the industry evolves, driven by technological advancements and shifting market demands, it's crucial for less common methods to be refined and potentially take a more prominent role.

The environmental and economic implications of these methods cannot be overstated. In a world increasingly conscious of ecological impacts and sustainability, the choice of extraction method is not solely a technical decision but also an ethical one. It's imperative for the industry to strike a delicate balance between operational efficiency, environmental responsibility, and economic viability. Techniques that minimize harmful emissions, reduce energy consumption, or use less hazardous chemicals might carry more weight in future considerations, even if they currently represent a smaller portion of the industry's practices. The adaptability of the lignin extraction industry to the burgeoning needs of various sectors, including bioplastics and biofuels, is a testament to its potential for growth and innovation. As demand for higher purity lignin increases, the industry is challenged to refine existing methods and explore new techniques that align with these evolving requirements.

REFERENCES

1. Alriols M. G., Tejado A., Blanco M. A., Mondragon I., and Labidi J., Agricultural palm oil tree residues as raw material for cellulose, lignin and hemicelluloses production by ethylene glycol pulping process/ Chemical Engineering Journal. 2009, Vol.148, №1, pp. 106-114
2. Chen S., Shen S., Mi X., Yan J., Wang G., Zhang J. and Zhou Y., Synthesis of surfactants from alkali lignin for enhanced oil recovery. Journal of Dispersion

Science and Technology. 2016, Vol.37, №11, pp. 1574-1580
3. DeBons F. E. Whittington novel lignin-based surfactant system for the Salem unit.SPE Annual Technical Conference and Exhibition, Dallas, Texas, October 6 – 9, 1991, pp.83-90
4. Fahma F., Iwamoto S., Hori N., Iwata T.and Takemura A., Isolation, preparation and characterization of nanofibers from oil palm empty-fruit-bunch (OPEFB) Cellulose. 2010, Vol.17, №5, pp. 977-985
5. Mazza D. Fu, G. and Tamaki Y., Lignin extraction from straw by ionic liquids and enzymatic hydrolysis of the cellulosic residues. Journal of Agricultural and Food Chemistry. 2010. Vol.58, №5, pp. 2915-2922
6. Garcia A., Alriols M. G., Llano-Ponte R. and Labidi J., Ultrasound-assisted fractionation of the lignocellulosic material. Bioresource Technology. 2011, Vol.102, №10, pp. 6326-6330
7. Harsono H., Putra A. S., Maryana R., Rizaluddin A. T., Hing Y. Y. , NakagawaIzumi A. and Ohi H., Preparation of dissolving pulp from oil palm empty fruit bunch by prehydrolysis soda-anthraquinone cooking method. Journal of Wood Science. 2016, Vol.62, №1, pp. 65-73
8. Ibrahim M. M. and Azian H., Extracting soda lignin from the black liquor of oil palm empty fruit bunch. Jurnal Teknologi. 2005,Vol.42, pp. 11-20
9. Ibrahim M. M., Nadiah M. N. and Azian H., Comparison studies between soda lignin and soda-anthraquinone lignin in terms of physic-chemical properties and structural features. Journal of Applied Sciences. 2006, Vol. 6, №2, pp. 292-296
10. Ibrahim M. M., Yusof N. M. and Hashim A., Comparison studies on soda lignin and soda anthraquinone lignin. The Malaysian Journal of Analytical Sciences. 2007, Vol.11, №1, pp. 206-212
11. Chemat F., Malaysian Palm Oil Board, Overview of the Malaysian Oil Palm Industry. 2009, Vol.1, №1, pp. 105-115
12. Maryana R., Rizaluddin A. T., reparation of dissolving pulp from oil palm Available:http:bepi.mpob.gov.my/images/overview/Overview_of_Industry_2015.pdf, October 1, 2016, pp. 20-22
13. Mason T. J., Vinatoru M., The extraction of natural products using ultrasound or microwaves. Current Organic Chemistry. 2011, Vol.15, №2, pp. 237-247
14. Mekhile S., R. Saidur, Safari A.and Mustaffa W. E., Biomass energy in Malaysia: current state and prospects.Renewable and Sustainable Energy Reviews. 2011, Vol.15, №7, pp. 3360-3370
15. Nazir M.S., Wahjoedi B. A., Yussof A. W. and Abdullah M. A., Eco-friendly extraction and characterization of cellulose from oil palm empty fruit bunches, BioResources. 2013. Vol. 8, №2, pp. 2161-2172
16. Pan X., Kadla J. F., Ehara K., Gilkes N. and Saddler J. N., Organically ethanol lignin from hybrid poplar as a radical scavenger: relationship between lignin structure, extraction conditions, and antioxidant activity, Journal of agricultural and food chemistry. 2006, Vol.54, №16, pp. 5806-5813
17. Rodrigues S. and Pinto G. A., Ultrasound extraction of phenolic compounds from coconut (Cocos nucifera) shell powder, Journal of Food Engineering. 2007, Vol.80, №3, pp. 869-872
18. Seng G. M., Awang M., Yi L.and Ani F. N., Production of pyrolytic oil for enhanced oil recovery, Proceedings of the 1st International Conference on Natural Resources Engineering & Technology, Putrajaya, Malaysia, July 24– 25, 2006

ISNN: print 2663-7006; online 2709-2666

19. Sun H., Liu Q., Chen S., Yan X., Dai L., Zhou Y.and Zhang J., Study on synthesis and performance of lignin polyether sulfonate surfactants for enhanced oil recovery, Journal of Dispersion Science and Technology. 2017, Vol.38, №8, pp. 1124-1128
20. Sun X. F., Sun R., Fowler P.and Baird M. S., Extraction and characterization of original lignin and hemicelluloses from wheat straw, Journal of Agricultural and Food Chemistry. 2005, Vol.53, №4, pp. 860-870
21. Suryo P. and Murachman B., Development of non-petroleum base chemicals for improving oil recovery in Indonesia, SPE Asia Pacific Oil and Gas Conference and Exhibition, Jakarta, Indonesia, April 17 – 19, 2001. pp. 60-70
22. Tan S. S., MacFarlane D. R., Upfal J., Edye L. A., Doherty W. O., Patti A. F. and Scott J. L., Extraction of lignin from lignocellulose at atmospheric pressure using alkyl benzenesulfonate ionic liquid, GreenChemistry. 2009, Vol.11, №3, pp. 339-345
23. Murachman B., U. S. Energy Information Administration (EIA), Malaysia, Available: http://www.eia.gov, October 1, 2016. pp. 10-24
24. Yunus R., Salleh S. F., Abdullah N.and Biak D. R. A., Effect of ultrasonic pre-treatment on low temperature acid hydrolysis of oil palm empty fruit bunch, BioresourceTechnology, 2010, Vol.101, №24, pp. 9792-9796
25. Zakzeski J., Weckhuysen B. M. Lignin solubilization and aqueous phase reforming for the production of aromatic chemicals and hydrogen. ChemSusChem. 2011,Vol.4, pp.369–378
26. Zeng J., Helms G. L., Gao X., Chen S., Quantification of wheat straw lignin structure by comprehensive NMR analysis. J. Agric. FoodChem. 61, 2013, pp.10848–10857
27. Thakur V. K., Thakur M. K., Raghavan P., Kessler M. R., Progress in green polymer composites from lignin for multifunctional applications: a review. ACS Sustain. ChemEng. 2014, Vol.2, pp.1072–1092
28. Wang M. C., Leitch M., Xu C. B., Synthesis of phenol-formaldehyde resol resins using organosolv pine lignins. EurPolym. J. 2009, Vol.45, pp.3380–3388
29. Wildschut J., Smit A. T, Reith J. H., Huijgen W. J. J., Ethanol-based organosolv fractionation of wheat straw for the production of lignin and enzymatically digestible cellulose. BioresourTechnol. 2013, Vol.135, pp.58–66
30. Bayerbach R., Meier D., Characterization of the water-insoluble fraction from fast pyrolysis liquids (pyrolytic lignin). Part IV: structure elucidation of oligomeric molecules. J. Anal. ApplPyrol. 2009,Vol.85, pp. 98–107
31. Capanema E. A., Balakshin M. Y., Kadla J. F., A comprehensive approach for quantitative lignin characterization by NMR spectroscopy. J. Agric. FoodChem. 2004, Vol.52, pp.1850–1860

ИССЛЕДОВАНИЕ РАЗЛИЧНЫХ МЕТОДОВ ИЗВЛЕЧЕНИЯ ЛИГНИНА ИЗ КОРЫ ДЕРЕВА

Л.З. Вазирова [0000-0003-0008-8973], И.Ф. Алакбарова
Азербайджанский Государственный Университет Нефти и Промышленности
vazirova.leyla@gmail.com

В этом исследовании изучаются различные методы извлечения лигнина из коры деревьев,

важного побочного продукта лесной и бумажной промышленности. Целью исследования является определение эффективных и устойчивых методов экстракции лигнина, который имеет потенциальное применение в биополимерах, производстве энергии и в качестве природного связующего. Мы оценили несколько методов экстракции, включая экстракцию растворителем, паровой взрыв и ферментативный гидролиз, уделяя особое внимание выходу, чистоте и воздействию на окружающую среду. Результаты показывают существенные различия в эффективности и устойчивости методов. Экстракция растворителем продемонстрировала высокую чистоту лигнина, но вызвала опасения по поводу окружающей среды. Паровой взрыв обеспечил баланс между выходом и экологичностью, в то время как ферментативный гидролиз оказался наиболее устойчивым, хотя и с более низким выходом. Это исследование способствует увеличению объема знаний об экстракции лигнина и его потенциальном промышленном применении, подчеркивая необходимость дальнейших исследований по оптимизации этих методов для коммерческого использования.
Ключевые слова: *лигнин, экстракция, кора дерева, растворитель, паровой взрыв, биополимеры.*

AĞAC QABIĞINDAN LİQNİNİN MÜXTƏLİF ÜSULLAR İLƏ ALINMASININ TƏDQİQİ

L.Z. Vəzirova [0000-0003-0008-8973], İ.F. Ələkbərova
Azərbaycan Dövlət Neft və Sənaye Universiteti
vazirova.leyla@gmail.com

Bu tədqiqat kağız sənayesinin mühüm əlavə məhsulu olan ağac qabığından liqninin alınmasının müxtəlif üsullarını araşdırır. Tədqiqatın məqsədi biopolimerlərdə, enerji istehsalında və təbii bağlayıcı kimi potensial tətbiqləri olan liqninin çıxarılması üçün səmərəli və etibarlı üsulları müəyyən etməkdir. Biz məhsuldarlığa, təmizliyə və ətraf mühitə təsirə diqqət yetirərək, həlledicinin çıxarılması, buxar partlayışı və enzimatik hidroliz daxil olmaqla bir neçə hasilat üsulunu qiymətləndirdik. Nəticələr metodların effektivliyi və möhkəmliyində əhəmiyyətli fərqləri göstərir. Solvent ekstraktı yüksək liqninin saflığını nümayiş etdirdi, lakin ekoloji narahatlıqları artırdı. Buxar partlayışı məhsuldarlıq və ətraf mühitə uyğunluq arasında tarazlığı təmin etdi, enzimatik hidroliz isə daha az məhsuldarlıqla da olsa, ən davamlı olduğunu sübut etdi. Bu tədqiqat lignin hasilatı və onun potensial sənaye tətbiqləri ilə bağlı artan biliklər toplusuna töhfə verir və bu metodların kommersiya istifadəsi üçün optimallaşdırılması üçün əlavə tədqiqatlara ehtiyacı vurğulayır.
Açar sözlər: *liqnin, ekstraksiya, ağac qabığı, solvent, buxar partlaması, biopolimerlər.*

ISNN: print 2663-7006; online 2709-2666

AJCN, Vol. 6, No. 1, 2024, pp. 54-63
https://doi.org/10.32010/AJCN04022024-54

UDC 541.13.544.65

ELECTROCHEMICAL REDUCTION OF ELEMENTAL SULFUR IN ETHYLENE GLYCOL ELECTROLYTE

N.Sh.Soltanova[0009-0007-0469-2365], R.H.Huseynova[0009-0004-5838-071X], V.A.Majidzade[0000-0001-5639-3104], A.O.Zeynalova[0009-0002-4639-7157], U.M.Gurbanova[0000-0001-6239-3207], A.Sh.Aliyev[0000-0003-0560-5263]
M.Nagiyev Institute of Catalysis and Inorganic Chemistry, Ministry of Science and Education of the Republic of Azerbaijan
nazli.az@mail.ru

The work is devoted to the study of the mechanism of reduction of elemental sulfur from ethylene glycol. For this purpose, linear and cyclic voltampere polarization curves were recorded. The influence of sulfur concentration in ethylene glycol electrolyte, potential unfolding rate and temperature on the sulfur reduction process was investigated. By recording the cyclic polarization curve, the range of potentials at which the reduction of elemental sulfur and its anodic oxidation occur was determined. It has been established that an increase in the concentration of sulfur in the electrolyte and temperature raises the speed of its reduction, and the process itself is controlled by the diffusion of sulfur ions to the cathode surface. In addition, the polarization curves on the platinum rotating disc electrode were recorded. The obtained data, namely the rectilinear dependence of i_p on the rotation speed of the electrode (ω) to the power of 0.5, confirm the proposal that the process of reduction of elemental sulfur is accompanied by diffusion polarization. The dependence of the current density on the rotation speed of the electrode to the power of 0.5 at different potentials showed that the process of reduction of elemental sulfur in non-aqueous ethylene glycol at potentials of (0.25÷0.4 V) is accompanied by diffusion polarization, whereas at potentials above 0.4 V, it is accompanied by electrochemical polarization.

Keywords : *Sulfur ions, electroreduction, polarization, scanrate.*

INTRODUCTION

Solar and wind energy have become alternatives to current fossil energy sources. However, realizing these energy sources requires efficient photoconverter batteries and storage systems. Such devices are mainly made on the basis of chalcogenide layers and their compounds with metals [1-8]. Among these devices, lithium-sulfur (Li-S) batteries have become promising storage devices due to their high theoretical energy intensity, low cost and low toxicity [9-12]. Therefore, the study of sulfur deposition and sulfur-based alloys is of interest to researchers. But electrodeposition was carried out most often using its compounds, rather than in its elemental form [13].

Electrochemical reduction of sulfur in organic solvents has been studied by different authors over the past 30 years [14-16]. In general, sulfur (S_8) reduction is carried out by various multielectron reactions, including the breaking of S-S bonds [17, 18]. The reduction of S_8 can be expressed as the transfer of 16 electrons, assuming a complete conversion, according to the following reaction:

$$S_8^0 + 2e^- \rightarrow S_8^{2-} \qquad (1)$$

The authors [19-23] believe that the electroreduction of sulfur occurs in two steps, although each is a multi-step process and may involve the formation of polysulfides with different chain lengths.

In [24,25], on the basis of theoretical studies, the authors suggested that S_4^{2-} and S_3^{2-} represent the shape of the chain. In another paper [26], the authors believe that the stable structure of polysulfides depends on the amount of n in S_n^{2-}, the chain structure is stable when n is less than five, and the cyclic structure is stable when the value of n is eight or nine. When n is six or seven, polysulfides can have both cyclic and chain forms.

The authors of the study [27] investigated the electroreduction of sulfur in N,N-dimethylformamide, anodic deposition in dimethyl sulfoxide (DMSO) [28], in acetonitrile [29] and in several aprotic solvents [30]. The reactions that occur in this case are usually chemically reversible, which makes it possible to use sulfur reduction as a cathode reaction for Li/S batteries.

In [31], sulfur was deposited on a carbon nanotube paper and elemental sulfur was precipitated (deposited) by electro-oxidation of a polysulfide solution ($\sim S_6^{2-}$).

The final goal of the work is the synthesis of metal sulfides with semiconductor properties from a non-aqueous ethylene glycol electrolyte. For this, it is necessary to study the electroreduction of elemental sulfur from the same electrolyte. Previously, the synthesis of metal sulfides with semiconductor properties was carried out from aqueous electrolytes with the participation of sodium sulfite [32].

EXPERIMENTAL PART

The studies were carried out in electrolytes containing ethylene glycol, ammonium chloride and elemental sulfur. Ammonium chloride was injected into the electrolyte to increase the electrical conductivity of the electrolyte, which is quite low in non-aqueous solutions. Cyclic and linear polarization curves were taken on the IVIUMSTAT Electrochemical Interface potentiostat. This made it possible to determine the potential region in which the reduction of sulfur ions occurs. Polarization studies were carried out in a three-electrode electrolyser, the working electrode was platinum with a surface area of 2 mm^2, the auxiliary electrode was platinum with a surface area of 4 cm^2, the reference electrode was the silver chloride; and all the potential values given in the table indicated relative to this electrode. In view of the fact that the viscosity of ethylene glycol is high and the solubility of sulfur in it is quite low, the electrolyte temperature was changed in the range of 353÷393 K. The temperature of the electrolyte during the electrolysis process was maintained using an ultra-universal thermostat UTU-4. Polarization curves were also recorded on a platinum rotating disc electrode with a diameter of 0.05 dm and an area of $2 \cdot 10^{-3}$ dm^2.

RESULTS AND DISCUSSION

Ethylene glycol is an organic compound with a very high polarity, and its dielectric constant at a temperature of 20°C is 37.7.

When the working electrode is immersed into the electrolyte, a stationary potential is established equal to E_{st} = 0.52 V. Figure 1 shows the general cyclic voltage curve of sulfur reduction in ethylene glycol. The figure shows that the reduction of elemental sulfur from ethylene glycol occurs in two stages, at potentials of +0.35V and -0.3V. The first plateau on the sulfur reduction curve at a potential of +0.4V corresponds to the adsorption of sulfur on the surface of the platinum cathode.

ISNN: print 2663-7006; online 2709-2666

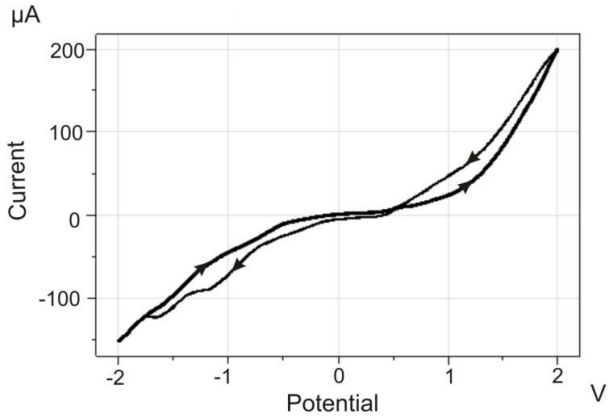

Fig.1. Cyclic polarization curve of sulfur electroreduction from ethylene glycol electrolyte on a platinum electrode. Electrolyte composition (M): S-0.001; NH_4Cl- 0.1; $C_2H_6O_2$; T=363K, υ =0.02 V/s

In all likelihood, adsorbed sulfur, having received 2 electrons, transforms into S_8^{2-}, and then, as a result of successive reactions (2) and (3), $2S_4^{2-}$ is formed, which is consistent with the data of [9].

$$S_8^{2-} + 2e^- \rightarrow S_8^{4-} \qquad (2)$$

$$S_8^{4-} \rightarrow 2S_4^{2-} \qquad (3)$$

The second peak at a potential of -1.2 V, the height of which is slightly higher than the height of the first plateau, corresponds to the reaction (4).

$$S_4^{2-} + 6e \rightarrow 4S^{2-} \qquad (4)$$

On the anodic component of the cyclic curve in the potential range 0.5÷1.0 V, either oxidation of under-reduced forms of sulfur, or oxidation of S^{2-} formed at the cathode occur.

Figure 2 shows the linear polarization curves of sulfur reduction from its concentration in the electrolyte. The sulfur concentration was changed in the range from 0.001 M to 0.005 M, while the stationary potential of the platinum electrode in the ethylene glycol sulfur solution did not change.

As the concentration of sulfur in the electrolyte increases, the height of these plateaus increases, i.e. an increase in the sulfur content in the electrolyte raises the rate of both processes. On the basis of these curves, the dependence of the height of the second current peak (i_p) corresponding to the reaction (3), on the concentration of sulfur in the electrolyte was plotted (fig.3). The rectilinearity of this relationship suggests that the limiting stage in the process of sulfur reduction is the dissociation of its ions.

Figure 4 shows the polarization curves of elemental sulfur reduction from ethylene glycol as a function of the potential unfolding rate.

The scan rate varied from 0.01 to 0.08 V/s.

As can be seen from the figure, an increase in the potential sweep rate contributes to the acceleration of sulfur adsorption, which is why, with an increase in the sweep rate, the height of the peak corresponding to the sulfur adsorption raises to a greater extent than the height of the peak corresponding to the reaction (4).

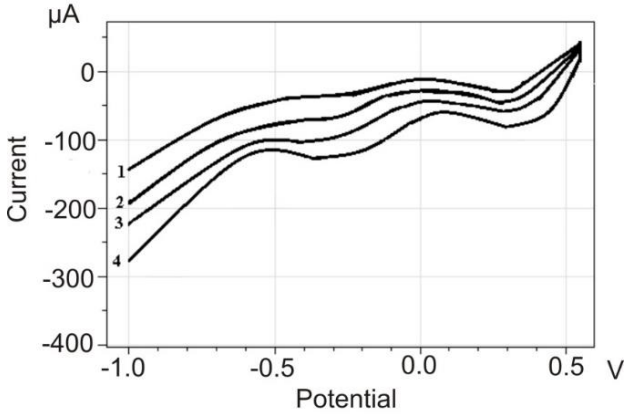

Fig.2. The effect of elemental sulfur concentration on its reduction in ethylene glycol electrolyte on a platinum electrode. Electrolyte composition (M): 0.1 NH_4Cl; $C_2H_6O_2$, S -1- 0.001; 2- 0.002; 3- 0.003; 4-0.005; υ = 0.02 V/s; T = 363 K

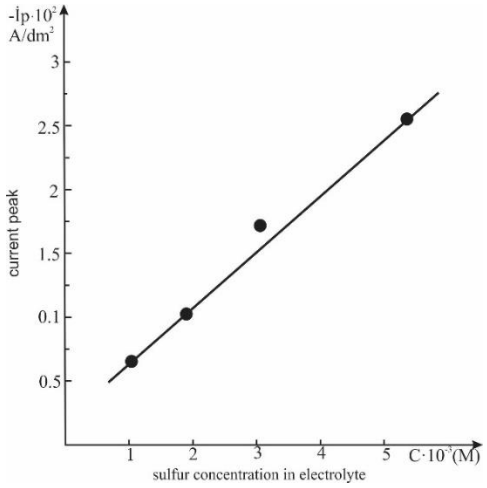

Fig.3. Dependence of current peak (i_p) on sulfur concentration in the electrolyte

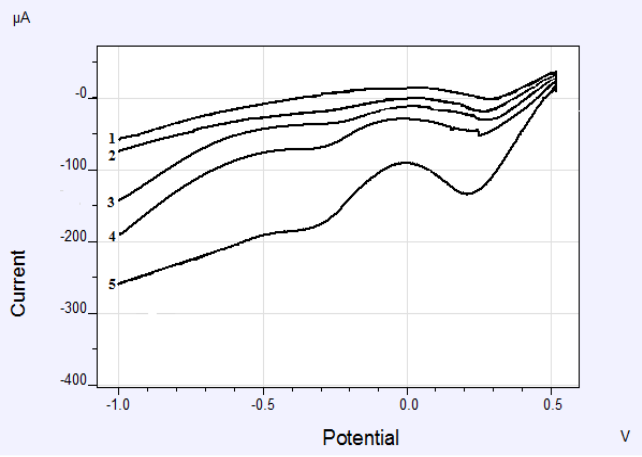

Fig.4. The polarization curve of elemental sulfur reduction from ethylene glycol as a function of potential sweep rate. Electrolyte composition (M): 0.001 S; 0.1 NH_4Cl; $C_2H_6O_2$; υ (V/sec): 1- 0.01; 2-0.02; 3- 0.04; 4 - 0.06; 5- 0.08; T = 363 K

ISNN: print 2663-7006; online 2709-2666

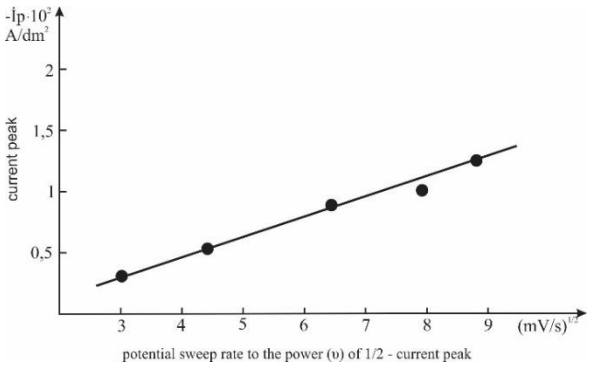

Fig.5. Dependence of the current peak on the potential sweep rate to the power of 1/2

An increase in the potential sweep rate amplifies the current for both sulfur reduction processes. Based on the data in figure 4, the $\sqrt{\upsilon}$ dependence of i_p (fig.5) was plotted. This relationship is rectilinear, which is also indicated by diffusion polarization in the reduction of sulfur from ethylene glycol.

In addition, the effect of temperature on the process of reduction of sulfur ions from ethylene glycol electrolyte was investigated. The temperature raise accelerates the process of sulfur reduction, so when the temperature rises from 353 K to 383 K, i.e. by 30 degrees, the speed of the process increases almost 4 times. A further increase in temperature to 393 K, as is seen from figure 6, does not affect the speed of the process. The temperature raise of the electrolyte accelerates the reduction process due to the fact that non-aqueous electrolytes are viscous and the reaction rate in them is usually limited by the diffusion stage, which accelerates with increasing temperature.

Linear polarization curves were also recorded on a platinum rotating disc electrode, as shown in figure 6. Increasing the rotational speed of the disc electrode accelerates the sulfur reduction process, as the dissociation process is accelerated.

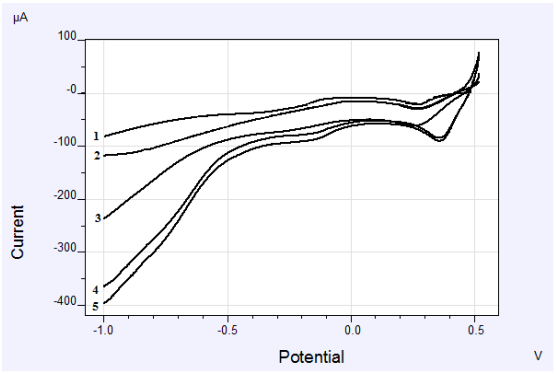

Fig.6. Polarization curves of reduction of elemental sulfur from ethylene glycol as a function of temperature. Electrolyte composition (M): 0.001 S, 0.1 NH_4Cl; $C_2H_6O_2$; υ = 0.02 V/s, T (K): 1 - 353; 2 - 363; 3 - 373; 4 - 383; 5 – 393

On the basis of fig.7, the dependence of the peak current on the rotation speed of the platinum disc electrode to the power of 1/2 is plotted (fig.8). This dependence for the sulfur reduction process is rectilinear, and its slope is characteristic of diffusion processes [33].

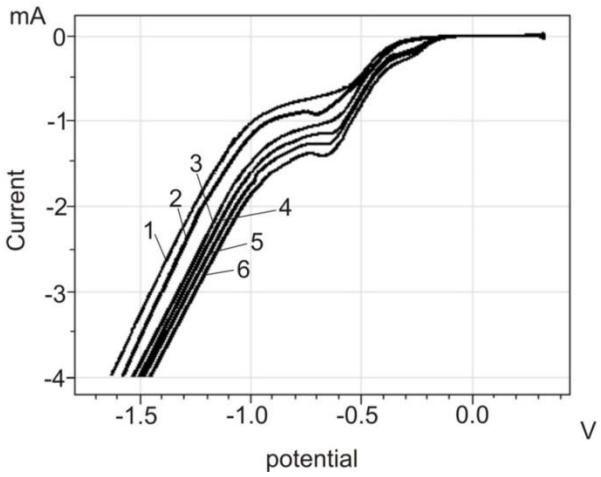

Fig.7. Linear polarization curves of sulfur reduction on a platinum rotating disc electrode. Electrolyte composition (M): S-0.001M, 0.1 NH_4Cl; $C_2H_6O_2$, υ = 0.02 V/s; T=363 K. Electrode rotation speed υ (rpm): 1-500, 2-1000, 3-2000, 4-3000, 5-4000, 6-5000

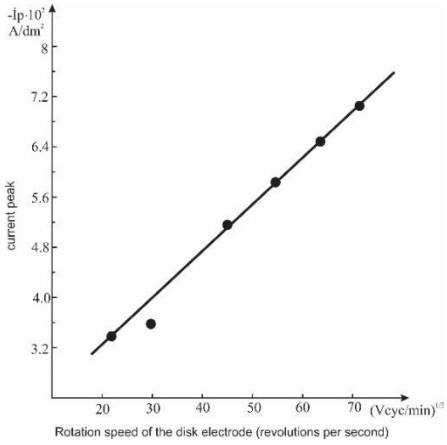

Fig. 8. Dependence of peak current (i_p) on the rotation speed of the electrode to the power of 1/2

In addition, from fig.7, the dependence of the current density on the rotation speed of the disk electrode at various potentials was also plotted, shown in figure 9.As can be seen from fig.9, an increase in the mixing intensity at cathode potentials from 0.25 V to 0.4 V has little effect on the rate of the cathode process. The weak effect of mixing intensity on the process rate indicates that at potentials up to 0.4 V, the limiting stage of the process is the transfer of discharged particles to the cathode surface, i.e., here, concentration polarization occurs.

When projecting these lines to the vertical axis, it can be seen that at cathode potentials from 0.25 V to 0.4 V, they cross the axis at zero, which is characteristic of processes where the limiting stage is the diffusion of deposited ions to the cathode surface.

ISNN: print 2663-7006; online 2709-2666

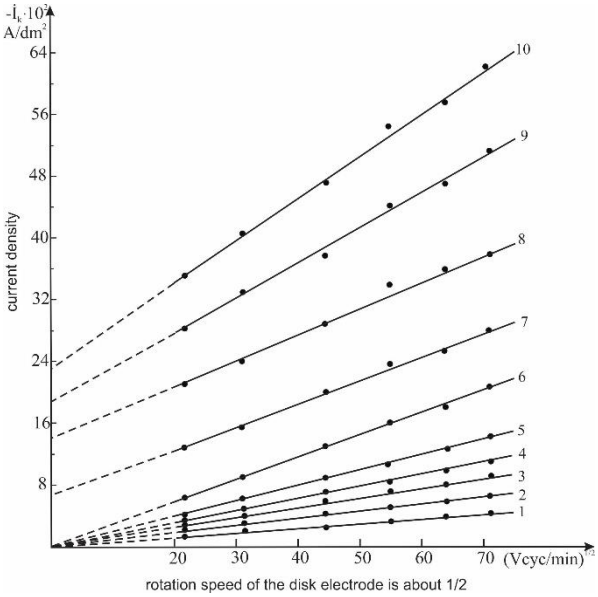

Fig. 9. Dependence of current density on the rotation speed of the disk electrode to the power of 1/2 (electrolyte composition as in figure 7), at potentials (V): 1-0.25; 2-0.3; 3-0.32; 4-0 .33; 6-0.4; 8-0.5;

At potentials of 0.45 V and above, the dependence of the reaction rate increases with the raise of the electrode rotation speed and the lines intersect the vertical axis above zero, which indicates that at high rotational speeds of the disc electrode, the determining stage is the electrochemical reaction of sulfur reduction [33].

CONCLUSION

By recording cyclic and linear polarization curves of elemental sulfur reduction in ethylene glycol, the range of potentials at which sulfur reduction occurs has been established. The influence of some factors, such as concentration of the sulfur ions in the electrolyte, the rate of potential unfolding and the temperature of the electrolyte on the reduction of sulfur ions was studied. From the dependence of the peak current on the sulfur concentration in the electrolyte and the potential scanrate, we can conclude that the reduction of sulfur is accompanied by diffusion kinetics. To confirm this conclusion, the polarization curves on the rotating disc electrode were recorded and the rectilinear structured i_p dependence was plotted, which is also inherent in processes controlled by diffusion. By graphing the dependence of the current density on the rotation speed of the disc electrode at different potentials, it was concluded that at the beginning of the reduction process of elemental sulfur in the potential range from 0.25 V to 0.4 V, the process is accompanied by concentration polarization, whereas at potentials from 0.45 V and higher - by electrochemical polarization.

REFERENCES

1. Javadova S.P., Majidzade V.A., Aliyev A.Sh., Azizova A.N., Tagiyev D.B. Electrodeposition of Bi-Se thin films involving ethylene glycol based electrolytes. J. Electrochem. Sci. and Eng. 2021, №11,pp. 51–58

2. Javadova S.P., Majidzade V.A., Aliyev A.Sh., Azizova A.N., Tagiyev D.B. Electrodeposition of Bi-Se thin films involving ethylene glycol based electrolytes. J. Electrochem. Sci. and Eng. 2021, №11,pp. 51–58
3. Shi Z., Zhang X., Lin X., Liu G., Ling Ch., Xi Sh. , Chen B., Ge Y., Tan Ch., Lai Zh., Zh.Huang, Ruan X., Zhai L., Li L., Li Z., Wang X., Nam G.-H., Liu J., He Q., Guan Z., Wang J., Lee Ch.-S., Kucernak A.R.J, Zhang H. Phase-dependent growth of Pt on MoS_2 for highly efficient H_2 evolution. Nature. 2023,Vol.621.pp. 300–305
4. Zeynalova A.O., Majidzade V.A., Javadova S.P., Aliyev A.Sh. Electrochemical synthesis of iron monoselenide thin films. Chem. Prob. 2021,Vol.19,№4,pp.262–271
5. Bozin E.S., Xie H., Abeykoon A.M.M., Everett S.M., Tucker M.G., Kanatzidis M.G., Billinge S.J.L. Local Sn Dipolar-Character Displacements behind the Low Thermal Conductivity in SnSe Thermoelectric. Phys. Rev. Lett. 2023,Vol.131, №3, pp.036101
6. Majidzade V.A., Aliyev A.Sh., Guliyev P.H., Babayev Y.N., Elrouby M., Tagiyev D.B. Electrochemical behaviour of selenite ions in tartaric electrolytes. J. Elec. Sci. and Eng. 2018, Vol.8, №3, pp.197–204
7. Majidzade V.A., Jafarova S.F., Javadova S.P., Aliyev A.Sh., Tagiyev D.B. The latest progress on synthesis and investigation of Sb_2S_3-based thin films. Chem. Prob. 2023, Vol.21, №2. pp. 99–122.
8. Majidzade V.A., Aliyev A.Sh., Guliyev P.H., Babanly D.M. Electrodeposition of the Sb_2Se_3 thin films on various substrates from the Tartaric electrolyte. Elec. Sci. and Eng. 2021, Vol.10, № 1, pp. 1–9
9. Imamaliyeva S.Z., Musayeva S.S., Babanly D.M., Jafarov Y.I., Taghiyev D.B., Babanly M.B. Determination of the thermodynamic functions of bismuth chalcoiodides by EMF method with morpholinium formate as electrolyte. Thermochimica Acta. 2019, Vol.679, pp. 178319
10. Zhan Y., Buffa A., Yu L., Xu Z.J., Mandler D. Electrodeposited Sulfur and Co_xS Electrocatalyst on Buckypaper as High-Performance Cathode for Li–S Batteries. Nano-Micro Letters. 2020, Vol.141, №12, pp. 1–13
11. Le P.-A., A general introduction to lithium-ion batteries: From the first concept to the top six commercials and beyond. J. Elec. Sci. and Eng. 2023, Vol.13, №4.pp. 591–604
12. Munawer M.E. Human health and environmental impacts of coal combustion and post-combustion wastes. J. Sustainable Mining 2018, Vol.17, №2, pp. 87–96
13. Mori R. Cathode materials for lithium-sulfur battery. J. Solid State Electrochemistry 2023, Vol.27, pp. 813–839
14. Jafarova S.F., Co-electrodeposition of thin Mo-S films. Azerbaijan Chemical Journal 2020, №1, pp. 16–19
15. Levillain E., Gaillard F., Demortie A.R, Lelieur J.P. Electrochemical and spectroelectrochemical study of the oxidation of S^{2-}_4 and S^{2-}_6 ions in liquid ammonia. J. Electroanal. Chem. 1996. Vol.405, pp. 85–94
16. Gaillard F., Levillain E. Visible time-resolved spectroelectrochemistry: application to study of the reduction of sulfur (S_8) in dimethylformamide. J. Electroanal. Chem. 1995, Vol.398, pp. 77–87
17. Levillain E., Gaillard F., Leghie P., Demortier A., Lelieur J.P. On the understanding of the reduction of sulfur (S_8) in dimethylformamide (DMF). J.

ISNN: print 2663-7006; online 2709-2666

Electroanal. Chem. 1997, Vol.420, pp. 167–177
18. Levillain E., Leghie P., Gobeltz N., Lelieur J.P. Identification of the S^{-4} Radical Anion in Solution. ChemInform. 2010, Vol.34, № 28, pp. 335-341
19. Chen R., Zhao T., Wu F. From a historic review to horizons beyond: lithium-sulphur batteries run on the wheels. Chem. Commun. 2015, Vol.51,pp. 18–33
20. Manan N.S.A., Aldous L., Alias Y., Murray P., Yellowlees L.J., Lagunas M.C., Hardacre C. Electrochemistry of sulfur and polysulfides in ionic liquids. J. Phys. Chem. 2011, Vol.115, № 47, pp.13873–13879
21. Zou Q., Lu Y.-C. Solvent-dictated lithium sulfur redox reactions: an operando UV–vis spectroscopic study. J. Phys. Chem. Lett. 2016, Vol.7, pp.1518–1525
22. Jeon B.H., Yeon J.H., Chung I.J. Preparation and electrical properties of lithium-sulfur-composite polymer batteries. J. Mat. Proces. Tech. 2003,Vol.143, pp.93–97
23. Jung Y., Kim S., Kim B.S., Han D.H., Park S.M., Kwak J. Effect of organic solvents and electrode materials on electrochemical reduction of sulfur. Int. J. Electrochem. Sci. 2008,Vol.3, pp.556–577
24. Moreno-Piza O.J., Suarez-Herrera M.F. Electrochemical study of the redox processes of elemental sulfur in organic solvents using poly (3,4-ethylene-dioxy-thiophene) modified glassy carbon electrodes as working electrodes and ionic liquids as electrolytes. Electrochimica Acta. 2022, Vol.436, pp.141442
25. Bosser G., Paris J., Plichon V. Stabilisation of nitrophenyl disulphide ions in dimethylacetamide, J. Chem. Soc. Chem. Commun. 1988, Vol.11, pp. 720–721
26. Salahub D.R., Foti A.E., Smith Jr V.H. Molecular orbital study of structural changes on oxidation and reduction of S_3, S_4, S_6 and S_8. J. Ame. Chem. Soc. 1978, Vol.100, pp.7847–7859
27. Ganteför G., Hunsicker S., Jones R.O. Prediction and observation of ring and chain isomers in S_n^- ions. Chem. Phys. Lett. 1995, Vol.236, pp.43–49
28. Han D.-H., Kim B.-S., Choi S.-J., Jung Y., Kwak J., Park S.-M. Time-Resolved In Situ Spectroelectrochemical Study on Reduction of Sulfur in N,N[sup ′]-Dimethylformamide. J. Electrochem. Soc. V. 151. Han, D.-H., Kim, B.-S., Choi, S.-J., Jung, Y., Kwak, J., & Park, S.-M. Time-Resolved In Situ Spectroelectrochemical Study on Reduction of Sulfur in N,N[sup ′]-Dimethylformamide. J. Elec. Soc. 2004, Vol.151, №9, pp.E283
29. Suni F. Li., Ian I. Electrodeposition of Elemental Sulfur from Dimethyl Sulfoxide (DMSO). J. Electrochem. Soc. 2018, Vol.165, №2, pp.D1-D5
30. Fujinaga T., Kuwamoto T., Okazaki S., Hojo M. Electrochemical Reduction of Elemental Sulfur in Acetonitrile. Bulletin of the Chemical Society of Japan. 1980, Vol.53, pp.2851–2855
31. Merritt M. V., Sawyer D. T. Electrochemical reduction of elemental sulfur in aprotic solvents. Formation of a stable S_8- species. Inorganic Chemistry. 1970, Vol.9, № 2, pp.211–215
32. Martin R.P., Doub W.H., Roberts J.L., Sawyer D.T. Electrochemical reduction of sulfur in aprotic solvents. Inorganic Chemistry. 1973, Vol.12, № 8, pp.1921–1925
33. Majidzade V.A., Cafarova S.F., Aliyev A.Sh., Farhatova N.B., Nuriyev Y.A., Tagiyev D.B. Electrochemical deposition of thin semiconductive Mo-S films. Aze. Chem. J. 2019, №1, pp.6–13
34. Yu.V. Pleskov, V.Yu. Filippovskiy, Rotating disc electrode. Nauka Publ., Moscow, Russia. 1972, pp.344

ЭЛЕКТРОХИМИЧЕСКОЕ ВОССТАНОВЛЕНИЕ ЭЛЕМЕНТАРНОЙ СЕРЫ В ЭТИЛЕНГЛИКОЛЕВОМ ЭЛЕКТРОЛИТЕ.

Н.Ш.Солтанова[0009-0007-0469-2365], Р.Г.Гусейнова[0009-0004-5838-071X],
В.А.Маджидзаде[0000-0001-5639-3104], А. О. Зейналова[0009-0002-4639-7157],
У.М.Курбанова[0000-0001-6239-3207], А.Ш.Алиев[0000-0003-0560-5263]
Институт Катализа и Неорганической Химии М.Нагиева, Министерства Науки и Образования Азербайджанской Республики
nazli.az@mail.ru

Работа посвящена исследованию механизма восстановления элементарной серы из этиленгликоля. Для этого были сняты линейные и циклические вольтамперные поляризационные кривые. Было исследовано влияние на процесс восстановления серы ее концентрации в этиленгликолевом электролите, скорости развертки потенциала и температуры. Снятием циклической поляризационный кривой определена область потенциалов, при которых происходит восстановление элементарной серы и ее анодное окисление. Установлено, что повышение концентрации серы в электролите и температуры увеличивает скорость процесса ее восстановления, а сам процесс контролируется диффузией ионов серы к поверхности катода. Кроме того, были сняты поляризационные кривые на вращающемся дисковом платиновом электроде. Полученные данные, а именно прямолинейная зависимость i_p от скорости вращения электрода (ω) в степени 0.5 подтверждают предложение, что процесс восстановления элементарной серы при низких потенциалах (0.25÷0.4 В) сопровождается диффузионной поляризацией, а при потенциалах выше 0.4 В сопровождается электрохимической поляризацией.
Ключевые слова:*ионы серы,электровосстановление,поляризация,скорость сканирования.*

ETİLENQLİKOL ELEKTROLİTİNDƏN ELEMENTAR KÜKÜRDÜN ELEKTROKİMYƏVİ REDUKSİYASI

N.Ş.Soltanova[0009-0007-0469-2365], R.Q.Hüseynova[0009-0004-5838-071X],
V.A.Məcidzadə[0000-0001-5639-3104], A.O.Zeynalova[0009-0002-4639-7157],
Ü.M.Qurbanova[0000-0001-6239-3207], A.Ş.Əliyev[0000-0003-0560-5263]
Azərbaycan Respublikası Elm və Təhsil Nazirliyi, Kataliz və Qeyri-üzvi Kimya İnstitutu
nazli.az@mail.ru

İş etilenqlikoldan elementar kükürdün alınması mexanizminin öyrənilməsinə həsr edilmişdir. Bu məqsədlə xətti və tsiklik voltaperometrik polyarizasiya əyriləri qeydə alınmışdır. Onun etilenqlikol elektrolitindəki qatılığının, potensial dəyişmə sürətinin və temperaturun kükürdün reduksiyası prosesinə təsiri tədqiq edilmişdir. Tsiklik polyarizasiya əyrisini qeyd etməklə elementar kükürdün reduksiyası və onun anodda oksidləşməsinin baş verdiyi potensiallar sahəsi müəyyən edilmişdir. Müəyyən edilmişdir ki, elektrolitdə və temperaturda kükürdün qatılığının artması onun reduksiya prosesinin sürətini artırır və prosesin özü kükürd ionlarının katod səthinə yayılması ilə idarə olunur. Bundan əlavə, polarizasiya əyriləri fırlanan platin disk elektrodunda qeydə alınıb. Əldə edilən məlumatlar, yəni ip-nin elektrodun fırlanma sürətindən (ω) 0.5 gücünə xətti asılılığı, aşağı potensiallarda (0.25÷0.4 V) elementar kükürdün reduksiya prosesinin diffuziya polyarizasiyası ilə müşayiət olunduğunu təsdiqləyir, 0.4 V-dan yuxarı potensiallarda isə elektrokimyəvi polarizasiya ilə müşayiət olunur.
Açar sözlər: *Kükürd ionları, elektroreduksiya, polyarizasiya, potensialın dəyişmə sürəti.*

ISNN: print 2663-7006; online 2709-2666

ATTENTION FOR AUTHORS!

"Azerbaijan Journal of Chemical News" approved by the Higher Attestation Commission under the President of Azerbaijan Republic and it is included to the list of journals and periodicals that should be published by major scientific results of dissertations in Azerbaijan Republic.